PWA 9 / ATHOS 4

Tools and Methods in Baryon Spectroscopy

Lothar Tiator
Johannes Gutenberg Universität Mainz

Bad Honnef, Germany, March 12, 2017

outline of my lecture:

- Introduction - Baryon resonances
- Breit-Wigner vs pole positions
- sources for resonance analyses
- formalism of 0^- photoproduction
- fixed-t dispersion relations
- Regge phenomenology
- dynamical models and isobar models
- fundamental properties of resonances
- poles, residues, photon decay amplitudes
- pole extraction methods
- poles on different Riemann sheets

Baryon resonances from PDG

from Review of Particle Physics 2016

(S, I)	(0, ½)	(0, 3/2)	(-1, 0)	(-1, 1)	(-2, ½)
	N	**Δ**	**Λ**	**Σ**	**Ξ**
all	27	22	17	25	10
****	11	7	8	5	1
***	4	3	5	4	4
**	10	7	1	7	2
*	2	5	3	9	3

**** Existence is certain, properties are at least fairly well explored.

*** Existence is very likely further confirmation of decay modes is required.

** Evidence of existence is only fair.

* Evidence of existence is poor.

27 Nucleon and 22 Delta resonances

Particle	J^P	overall	Status as seen in $N\gamma$	$N\pi$	$N\eta$	$N\sigma$	$N\omega$	ΛK	ΣK	$N\rho$	$\Delta\pi$
N	$1/2^+$	****									
$N(1440)$	$1/2^+$	****	****	****		***				*	***
$N(1520)$	$3/2^-$	****	****	****	***					***	***
$N(1535)$	$1/2^-$	****	****	****	****					**	*
$N(1650)$	$1/2^-$	****	****	****	***			***	**	**	***
$N(1675)$	$5/2^-$	****	****	****	*			*		*	***
$N(1680)$	$5/2^+$	****	****	****	*	**				***	***
$N(1700)$	$3/2^-$	***	**	***	*			*	*	*	***
$N(1710)$	$1/2^+$	****	****	****	***		**	****	**	*	**
$N(1720)$	$3/2^+$	****	****	****	***			**	**	**	*
$N(1860)$	$5/2^+$	**		**						*	*
$N(1875)$	$3/2^-$	***	***	*			**	***	**		***
$N(1880)$	$1/2^+$	**	*	*		**		*			
$N(1895)$	$1/2^-$	**	**	*	**			**	*		
$N(1900)$	$3/2^+$	***	***	**	**		**	***	**	*	**
$N(1990)$	$7/2^+$	**	**	**					*		
$N(2000)$	$5/2^+$	**	**	*	**			**	*	**	
$N(2040)$	$3/2^+$	*		*							
$N(2060)$	$5/2^-$	**	**	**	*				**		
$N(2100)$	$1/2^+$	*		*							
$N(2120)$	$3/2^-$	**	**	**				*	*		
$N(2190)$	$7/2^-$	****	***	****			*	**		*	
$N(2220)$	$9/2^+$	****		****							
$N(2250)$	$9/2^-$	****		****							
$N(2300)$	$1/2^+$	**		**							
$N(2570)$	$5/2^-$	**		**							
$N(2600)$	$11/2^-$	***		***							
$N(2700)$	$13/2^+$	**		**							

**** Existence is certain, and properties are at least fairly well explored.

*** Existence is very likely but further confirmation of decay modes is required.

** Evidence of existence is only fair.

* Evidence of existence is poor.

Particle	J^P	overall	Status as seen in $N\gamma$	$N\pi$	$N\eta$	$N\sigma$	$N\omega$	ΛK	ΣK	$N\rho$	$\Delta\pi$
$\Delta(1232)$	$3/2^+$	****	****	****	F						
$\Delta(1600)$	$3/2^+$	***	***	***	o					*	***
$\Delta(1620)$	$1/2^-$	****	***	****	r					***	***
$\Delta(1700)$	$3/2^-$	****	****	****	b					**	***
$\Delta(1750)$	$1/2^+$	*		*	i						
$\Delta(1900)$	$1/2^-$	**	**	**	d			**	**	**	
$\Delta(1905)$	$5/2^+$	****	****	****	d			***	**	**	
$\Delta(1910)$	$1/2^+$	****	**	****	e			*	*	**	
$\Delta(1920)$	$3/2^+$	***	**	***	n			***		**	
$\Delta(1930)$	$5/2^-$	***		***							
$\Delta(1940)$	$3/2^-$	**	**	*	F						
$\Delta(1950)$	$7/2^+$	****	****	****	o			***	*	***	
$\Delta(2000)$	$5/2^+$	**			r					**	
$\Delta(2150)$	$1/2^-$	*		*	b						
$\Delta(2200)$	$7/2^-$	*		*	i						
$\Delta(2300)$	$9/2^+$	**		**	d						
$\Delta(2350)$	$5/2^-$	*		*	d						
$\Delta(2390)$	$7/2^+$	*		*	e						
$\Delta(2400)$	$9/2^-$	**		**	n						
$\Delta(2420)$	$11/2^+$	****	*	****							
$\Delta(2750)$	$13/2^-$	**		**							
$\Delta(2950)$	$15/2^+$	**		**							

$N(1440)1/2^+$ was $P_{11}(1440)$
$\Delta(1232)3/2^+$ was $P_{33}(1232)$
$N(1520)3/2^-$ was $D_{13}(1520)$
$\Delta(1700)3/2^-$ was $D_{33}(1700)$
etc.

how to describe baryon resonances

quark models	static ($q\bar{q}$, qqq), spectrum dynamical, form factors, decays
lattice QCD	static ($q\bar{q}$, qqq), spectrum dynamical, Lüscher's method, phase-shifts
dynamical models	bare resonances (e.g. qqq) meson-baryon dynamics –> dressed resonances in some cases even without a bare state –> dynamically generated resonances
isobar models	Breit-Wigner ansatz, sometimes very simple sometimes very sophisticated inspired by the dynamical models
pole ansatz	Laurent series instead of Breit-Wigner are most general 1st order singularities (poles) are the resonance states residues are the elastic and inelastic amplitudes most general ansatz: Laurent+Pietarinen

Breit-Wigner
vs
Pole Positions

theoretical poles and experimental bumps

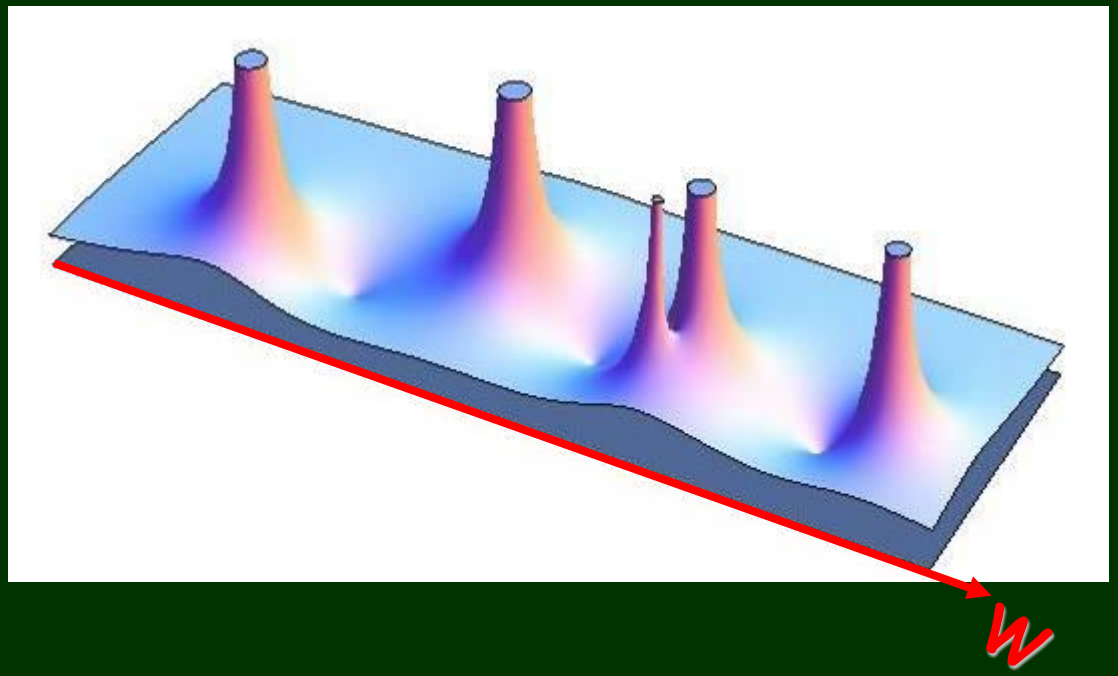

poles in the
complex plane

bumps on the
physical axis

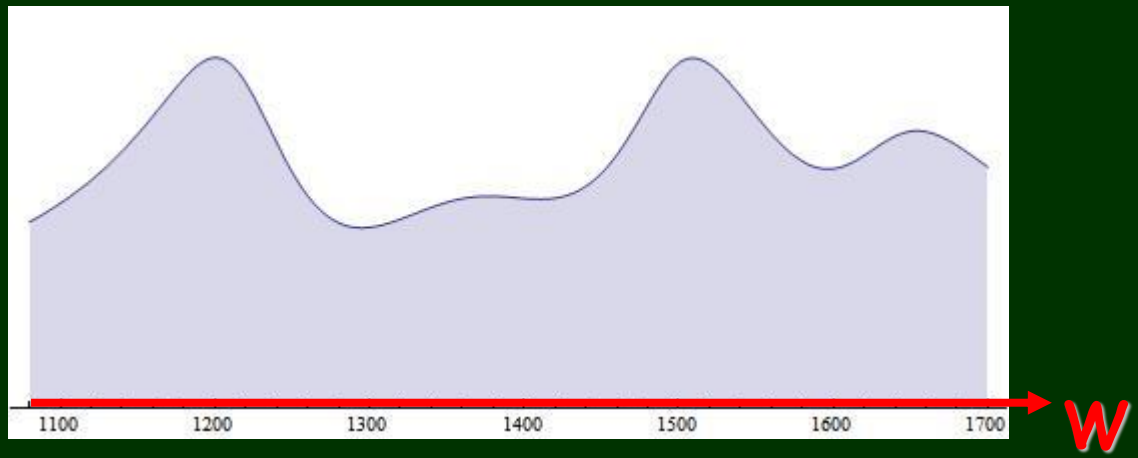

poles in the P_{33} and P_{11} partial waves

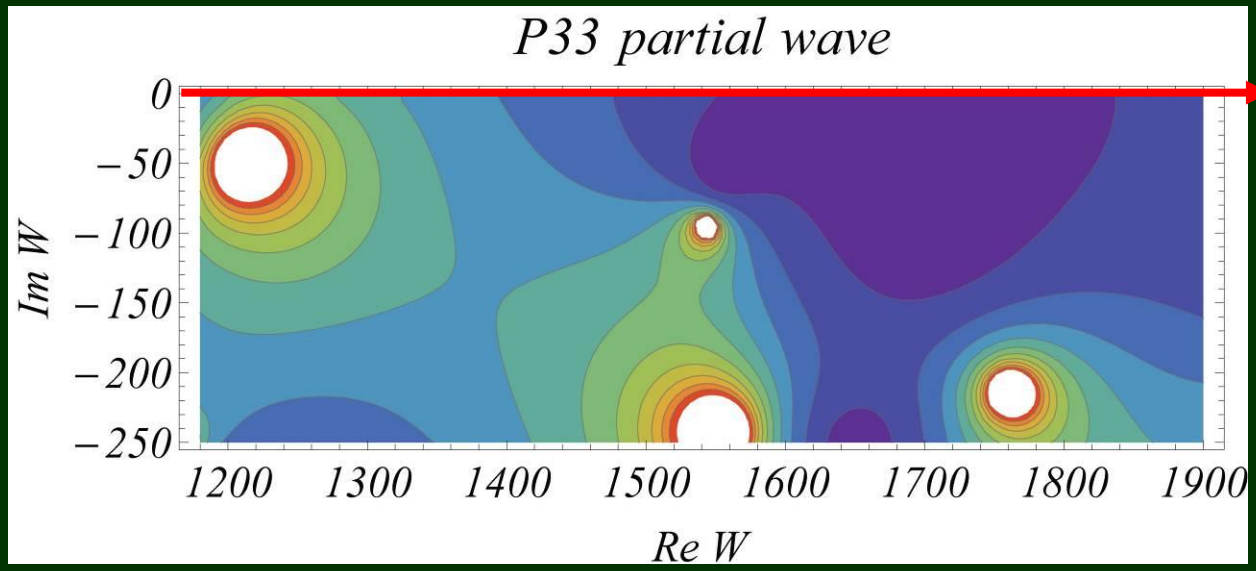

$P_{33}(1232)$

$P_{33}(1600)$

$P_{33}(XXX)$

$P_{33}(1920)$

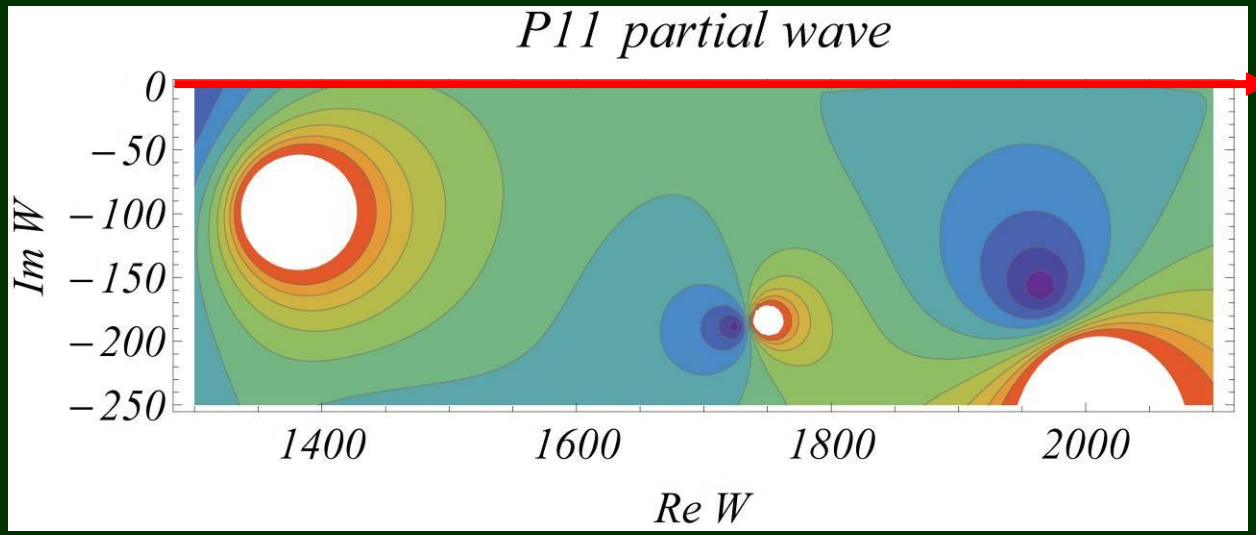

$P_{11}(1440)$

$P_{11}(1710)$

$P_{11}(2100)$

pole structure found in the Dubna-Mainz-Taipei model DMT2007

Formalism

of pseudoscalar meson photoproduction

- reactions
- kinematics
- amplitudes
- multipoles (partial-wave amplitudes)
- cross section and polarization observables

Sources for Baryon resonance analysis

$\pi N \rightarrow \pi N$ pion elastic scattering: by far most important

$\pi N \rightarrow X$ pion inelastic scattering

$\gamma N \rightarrow \pi N, K\Lambda, \eta N, \ldots$ photo- and electroproduction

$pp \rightarrow p\bar{p}\pi, pp\eta, \ldots$ nucleon-nucleon scattering

$J/\Psi \rightarrow pp\pi, \ldots$ J/Ψ and Ψ' decays in e^+e^-

SU(3) Flavour

Baryon Octett

$J^P = ½^+$

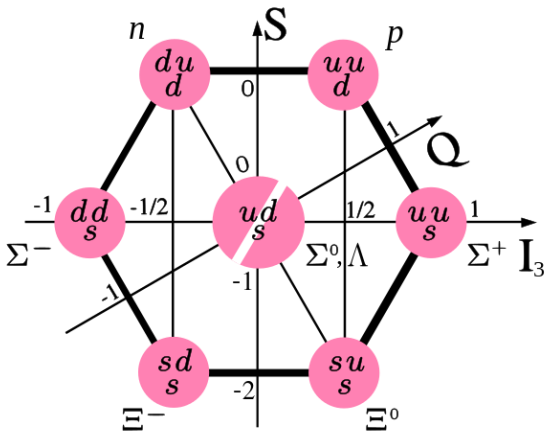

Meson Nonett

$J^P = 0^-$

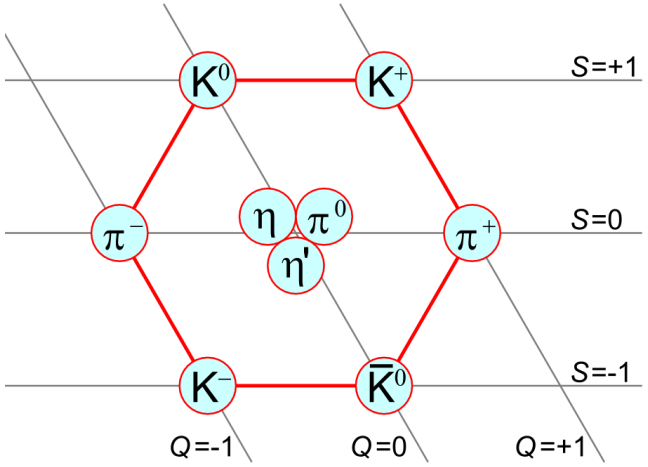

14 reactions:

γp	$\rightarrow$	$p\,\pi^0$	γn	$\rightarrow$	$n\,\pi^0$
		$n\,\pi^+$			$p\,\pi^-$
		$\Lambda\,K^+$			$\Lambda\,K^0$
		$\Sigma^0\,K^+$			$\Sigma^0\,K^0$
		$\Sigma^+\,K^0$			$\Sigma^-\,K^+$
		$p\,\eta$			$n\,\eta$
		$p\,\eta'$			$n\,\eta'$

Kinematics

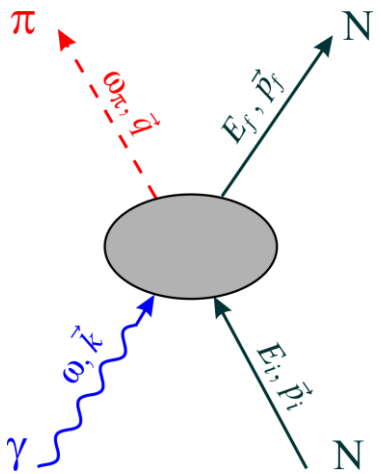

s-channel: $\gamma + N \rightarrow \pi + N$

u-channel: $\pi + N \rightarrow \gamma + N$

t-channel: $N + \bar{N} \rightarrow \pi + \gamma$

Mandelstam variables

$$
\begin{aligned}
s &= (p_i + k)^2 = (p_f + q)^2 \\
t &= (q - k)^2 = (p_f - p_i)^2 \\
u &= (p_i - q)^2 = (p_f - k)^2
\end{aligned}
$$

$$s + t + u = 2M_N^2 + M_\pi^2$$

Mandelstam plane

t-channel: $N + \bar{N} \to \pi + \gamma$

starts at $t = 4\,M_N^{\,2}$

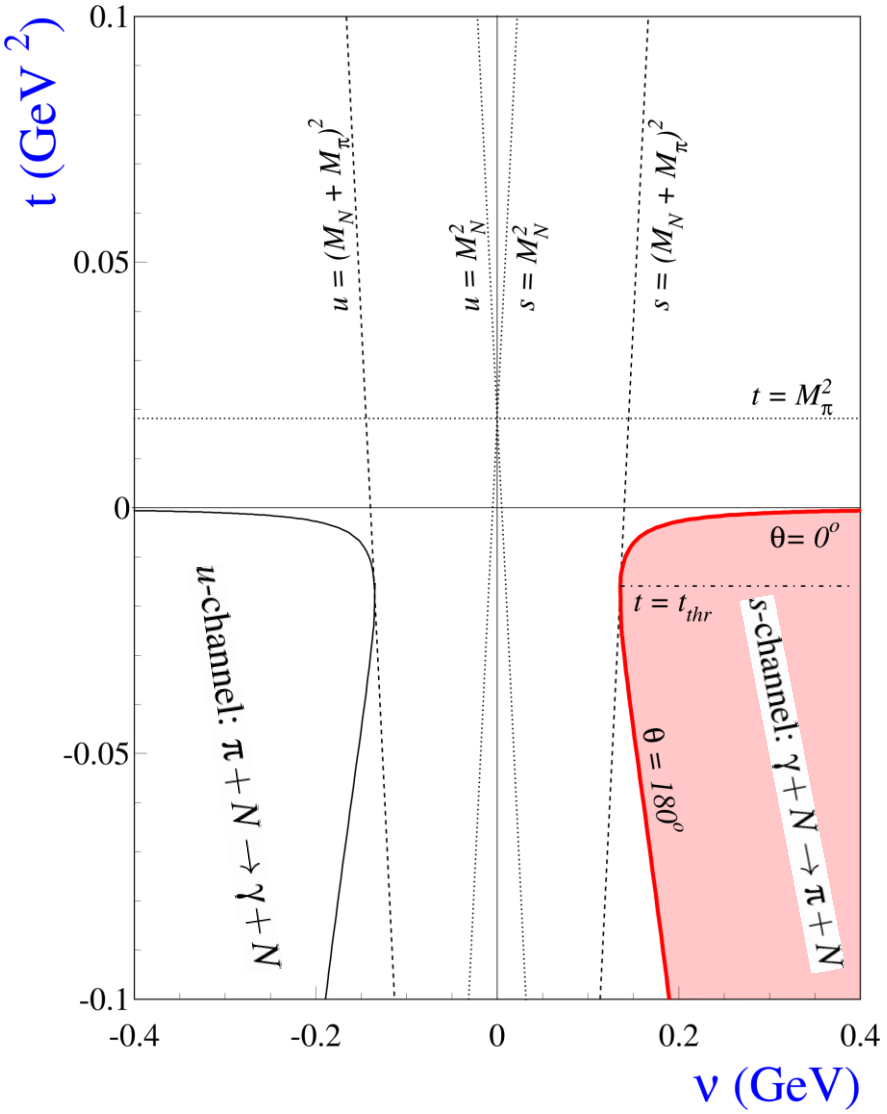

crossing variable:

$$\nu = (s-u)/4M_N$$

nucleon poles at:

$$s = M_N^2 \quad \text{or} \quad \nu_s = \nu_B$$

$$u = M_N^2 \quad \text{or} \quad \nu_u = -\nu_B \quad \text{with} \quad \nu_B = (t - M_\pi^2)/4M_N$$

thresholds at:

$$s = (M_N^2 + M_\pi)^2$$

$$u = (M_N^2 + M_\pi)^2$$

kinematical boundaries at θ=0° and θ=180° :

$$\cos\theta = \frac{(s-M_N^2) - M_\pi^2(s+M_N^2) + 2st}{2q\sqrt{s}(s-M_N^2)}$$

$$s = M_N(M_N + 2\nu) - \frac{1}{2}(t - M_\pi^2)$$

Fixed-t dispersion relations

from Höhler's bible (Landolt-Börnstein, 1983, p. 533f)

using crossing symmetry and Schwarz reflection theorem:

$$B^{\pm}(\nu + i0, t) = \mp B^{\pm}(-\nu - i0, t) = \mp B^{\pm *}(-\nu + i0, t)$$

one obtains for isospin even/odd invariant πN amplitudes $B^{\pm}(\nu, t)$:

$$\mathrm{Re}B^{\pm}(\nu, t) = B_N^{\pm}(\nu, t) + \frac{1}{\pi} \mathcal{P} \int_{\nu_{thr}}^{\infty} \mathrm{d}\nu' \, \mathrm{Im}B^{\pm}(\nu' + i0, t) \left(\frac{1}{\nu' - \nu} \mp \frac{1}{\nu' + \nu} \right)$$

with nucleon pole terms:

$$B_N^{\pm}(\nu, t) = \frac{g^2}{2M_N} \left(\frac{1}{\nu_B - \nu} \mp \frac{1}{\nu_B + \nu} \right)$$

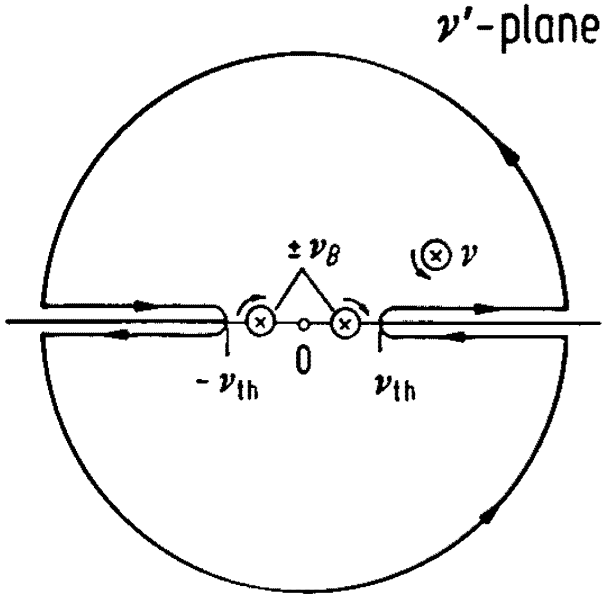

Fig. A.6.7. Contour of integration in the complex ν'-plane. If Cauchy's theorem is written for the function $B(\nu', t)/(\nu' - \nu)$ at fixed t over the small circle around ν, and the contour is blown up as shown in this figure, one obtains the dispersion relation (A.6.30), if ν is chosen real and Eq. (A.6.16) is used.

number of independent amplitudes in a specific reaction

The number of amplitudes, invariant amplitudes or spin or helicity amplitudes etc. depends on the spin degrees of freedom and C P T symmetries:

reaction	spin degrees	reduced by parity
$\pi\ \pi \rightarrow \pi\ \pi$	$1\otimes1 \otimes 1\otimes1$	1
$\pi\ N \rightarrow \pi\ N$	$1\otimes2 \otimes 1\otimes2$	2
$\gamma\ N \rightarrow \pi\ N$	$2\otimes2 \otimes 1\otimes2$	4
$\gamma^*\ N \rightarrow \pi\ N$	$3\otimes2 \otimes 1\otimes2$	6

Invariant amplitudes of pseudoscalar photoproduction

The nucleon e.m. current can be expressed in terms of 4 invariant amplitudes:

$$J^\mu = \sum_{i=1}^{4} A_i(\nu, t)\, M_i^\mu$$

$$\begin{aligned}
M_1^\mu &= -\frac{1}{2} i\gamma_5 \left(\gamma^\mu k - k\gamma^\mu\right) \\
M_2^\mu &= 2i\gamma_5 \left(P^\mu k\cdot(q-\frac{1}{2}k) - (q-\frac{1}{2}k)^\mu k\cdot P \right) \\
M_3^\mu &= -i\gamma_5 \left(\gamma^\mu k\cdot q - k q^\mu\right) \\
M_4^\mu &= -2i\gamma_5 \left(\gamma^\mu k\cdot P - k P^\mu\right) - 2M_N M_1^\mu
\end{aligned} \qquad P^\mu = (p_i^\mu + p_f^\mu)/2$$

advantages:

lorentz invariance

gauge invariance

crossing symmetry

easily obtained in field-theoretical models by Feynman diagrams

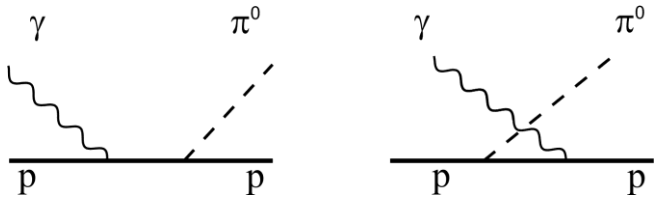

Isospion and crossing symmetry

The crossing symmetry of the invariant amplitudes depends on the isospin.

For π^0 and η photoproduction A_1, A_2, A_4 are crossing symmetric A_3 is antisymmetric.

For π photoproduction, the IA can be decomposed into 3 isospin channels $a=1,2,3$:

$$A_i^a = A_i^{(-)} i\varepsilon^{a3b}\tau^b + A_i^{(0)}\tau^a + A_i^{(+)}\delta_{a3}$$

and fulfil the following crossing relations:

$$\begin{aligned} A_i^{(0,+)}(-\nu,t) &= A_i^{(0,+)}(\nu,t) \quad i=1,2,4, & A_3^{(0,+)}(-\nu,t) &= -A_3^{(0,+)}(\nu,t) \\ A_i^{(-)}(-\nu,t) &= -A_i^{(-)}(\nu,t) \quad i=1,2,4, & A_3^{(-)}(-\nu,t) &= A_3^{(-)}(\nu,t) \end{aligned}$$

The physical photoproduction amplitudes are obtained by linear combinations:

$$\begin{aligned} A_i(\gamma p \to n\pi^+) &= \sqrt{2}(A_i^{(-)} + A_i^{(0)}) \\ A_i(\gamma p \to p\pi^0) &= A_i^{(+)} + A_i^{(0)} \\ A_i(\gamma n \to p\pi^-) &= -\sqrt{2}(A_i^{(-)} - A_i^{(0)}) \\ A_i(\gamma n \to n\pi^0) &= A_i^{(+)} - A_i^{(0)} \end{aligned}$$

Fixed-*t* dispersion relations in photoproduction

e.g. Pasquini, Drechsel, Tiator, EPJ A27 (2006) 231 and A34 (2007) 387

for crossing even amplitudes: $I = +, 0$ and $i = 1,2,4$ and also $I = -$ and $i = 3$

$$\mathrm{Re}A_i^{(I)}(\nu,t) = A_i^{(I)\,pole}(\nu,t) + \frac{2}{\pi}\,\mathcal{P}\!\int_{\nu_{thr}}^{\infty} d\nu'\,\frac{\nu'\,\mathrm{Im}A_i^{(I)}(\nu',t)}{\nu'^2-\nu^2}$$

for crossing odd amplitudes: $I = +, 0$ and $i = 3$ and also $I = -$ and $i = 1,2,4$

$$\mathrm{Re}A_i^{(I)}(\nu,t) = A_i^{(I)\,pole}(\nu,t) + \frac{2\nu}{\pi}\,\mathcal{P}\!\int_{\nu_{thr}}^{\infty} d\nu'\,\frac{\mathrm{Im}A_i^{(I)}(\nu',t)}{\nu'^2-\nu^2}$$

with better convergence for crossing odd amplitudes

CGLN amplitudes and multipoles

The matrix element of the e.m. current can be decomposed with Pauli spinors in spin space and expanded into the CGLN amplitudes in the cm frame with Coulomb gauge.

$$t_{\gamma,\pi} = \bar{u}(p_f) \sum_{i=1}^{4} A_i \varepsilon_\mu M_i^\mu u(p_i) = -\frac{4\pi W}{M_N} \chi_f^\dagger \mathcal{F} \chi_i$$

$$\begin{aligned} \mathcal{F} &= -\varepsilon_\mu J_{\pi N}^\mu \\ &= i(\vec{\sigma}\cdot\hat{\varepsilon})F_1 + (\vec{\sigma}\cdot\hat{q})(\vec{\sigma}\times\hat{k})\cdot\hat{\varepsilon}F_2 + i(\hat{\varepsilon}\cdot\hat{q})(\vec{\sigma}\cdot\hat{k})F_3 + i(\hat{\varepsilon}\cdot\hat{q})(\vec{\sigma}\cdot\hat{q})F_4 \end{aligned}$$

The CGLN can be expanded into electric and magnetic multipoles, which are the partial waves of photoproduction.

$$\begin{aligned} F_1 &= \sum_{l=0}^{\infty} [(lM_{l+} + E_{l+})P'_{l+1}(x) + ((l+1)M_{l-} + E_{l-})P'_{l-1}(x)] \\ F_2 &= \sum_{l=1}^{\infty} [(l+1)M_{l+} + lM_{l-}]P'_l(x) \\ F_3 &= \sum_{l=1}^{\infty} [(E_{l+} - M_{l+})P''_{l+1}(x) + (E_{l-} + M_{l-})P''_{l-1}(x)] \\ F_4 &= \sum_{l=2}^{\infty} [M_{l+} - E_{l+} - M_{l-} - E_{l-}]P''_l(x) \end{aligned}$$

Multipole projections

From the CGLN expansion one obtains the following multipole projections:

$$
\begin{aligned}
E_{l+} &= \int_{-1}^{1} dx \left[\frac{1}{2(l+1)} P_l F_1 - \frac{1}{2(l+1)} P_{l+1} F_2 + \frac{1}{2(l+1)} \frac{l}{2l+1} (P_{l-1} - P_{l+1}) F_3 \right. \\
&\quad \left. + \frac{1}{2(2l+3)} (P_l - P_{l+2}) F_4 \right] \\
E_{l-} &= \int_{-1}^{1} dx \left[\frac{1}{2l} P_l F_1 - \frac{1}{2l} P_{l-1} F_2 + \frac{l+1}{2l(2l+1)} (P_{l+1} - P_{l-1}) F_3 \right. \\
&\quad \left. + \frac{1}{2(2l-1)} (P_l - P_{l-2}) F_4 \right] \\
M_{l+} &= \int_{-1}^{1} dx \left[\frac{1}{2(l+1)} P_l F_1 - \frac{1}{2(l+1)} P_{l+1} F_2 + \frac{1}{2(l+1)(2l+1)} (P_{l+1} - P_{l-1}) F_3 \right] \\
M_{l-} &= \int_{-1}^{1} dx \left[-\frac{1}{2l} P_l F_1 + \frac{1}{2l} P_{l-1} F_2 + \frac{1}{2l(2l+1)} (P_{l-1} - P_{l+1}) F_3 \right]
\end{aligned}
$$

For S and P waves, some multipoles are forbidden,
in total, for a given $L_{\max} > 0$ we get $4\,L_{\max}$ multipoles, in detail, these are:

$$E_{0+},,,,E_{1+},,M_{1+},M_{1-},E_{2+},E_{2-},M_{2+},M_{2-},\ldots$$

Helicity and transversity amplitudes

The CGLN amplitudes and multipoles are uniquely defined in the literature.

Helicity and Transversity amplitudes depend on phase conventions
and have different sequences or names in the literature.

Here we use the definitions and conventions of Walker 1969 and Barker 1975

$$
\begin{aligned}
H_1 &= -\frac{1}{\sqrt{2}}\sin\theta\cos\frac{\theta}{2}\,(F_3+F_4)\\
H_2 &= \sqrt{2}\cos\frac{\theta}{2}\,[(F_2-F_1)+\frac{1-\cos\theta}{2}(F_3-F_4)]\\
H_3 &= \frac{1}{\sqrt{2}}\sin\theta\sin\frac{\theta}{2}\,(F_3-F_4)\\
H_4 &= \sqrt{2}\sin\frac{\theta}{2}\,[(F_1+F_2)+\frac{1+\cos\theta}{2}(F_3+F_4)]
\end{aligned}
$$

Helicity amplitudes
are the matrix elements
of the e.m. current
with the spin quantized
along the photon and pion momenta

Transversity amplitudes
use a spin quantization
transverse to the reaction plane

They have the following interesting
symmetry:

$$b_2(\theta) = -b_1(-\theta) \quad \text{and} \quad b_4(\theta) = -b_3(-\theta)$$

$$
\begin{aligned}
b_1 &= \frac{1}{2}[(H_1+H_4)+i\,(H_2-H_3)]\\
b_2 &= \frac{1}{2}[(H_1+H_4)-i\,(H_2-H_3)]\\
b_3 &= \frac{1}{2}[(H_1-H_4)-i\,(H_2+H_3)]\\
b_4 &= \frac{1}{2}[(H_1-H_4)+i\,(H_2+H_3)]
\end{aligned}
$$

16 polarization observables expressed in amplitudes

with helicity and transversity amplitudes the observables can be very conveniently expressed:

Again care must be taken!

We use definitions and conventions of Walker 1969 and Barker 1975

see also:
A Rosetta Stone ...
Sandorfi et al,
arXiv:1108.5411

Observable	Helicity representation	Transversity representation	Type
I	$\frac{1}{2}\,(\lvert H_1\rvert^2+\lvert H_2\rvert^2+\lvert H_3\rvert^2+\lvert H_4\rvert^2)$	$\frac{1}{2}(\lvert b_1\rvert^2+\lvert b_2\rvert^2+\lvert b_3\rvert^2+\lvert b_4\rvert^2)$	
$\check{\Sigma}$	$\mathrm{Re}(H_1H_4^*-H_2H_3^*)$	$\frac{1}{2}(\lvert b_1\rvert^2+\lvert b_2\rvert^2-\lvert b_3\rvert^2-\lvert b_4\rvert^2)$	S
$\check{T}$	$\mathrm{Im}(H_1H_2^*+H_3H_4^*)$	$\frac{1}{2}(\lvert b_1\rvert^2-\lvert b_2\rvert^2-\lvert b_3\rvert^2+\lvert b_4\rvert^2)$	
$\check{P}$	$-\mathrm{Im}(H_1H_3^*+H_2H_4^*)$	$\frac{1}{2}(\lvert b_1\rvert^2-\lvert b_2\rvert^2+\lvert b_3\rvert^2-\lvert b_4\rvert^2)$	
$\check{G}$	$-\mathrm{Im}(H_1H_4^*+H_2H_3^*)$	$\mathrm{Im}(b_1b_3^*+b_2b_4^*)$	
$\check{H}$	$-\mathrm{Im}(H_1H_3^*-H_2H_4^*)$	$\mathrm{Re}(b_1b_3^*-b_2b_4^*)$	BT
$\check{E}$	$\frac{1}{2}(-\lvert H_1\rvert^2+\lvert H_2\rvert^2-\lvert H_3\rvert^2+\lvert H_4\rvert^2)$	$-\mathrm{Re}(b_1b_3^*+b_2b_4^*)$	
$\check{F}$	$\mathrm{Re}(H_1H_2^*+H_3H_4^*)$	$\mathrm{Im}(b_1b_3^*-b_2b_4^*)$	
$\check{O}_x$	$-\mathrm{Im}(H_1H_2^*-H_3H_4^*)$	$-\mathrm{Re}(b_1b_4^*-b_2b_3^*)$	
$\check{O}_z$	$\mathrm{Im}(H_1H_4^*-H_2H_3^*)$	$-\mathrm{Im}(b_1b_4^*+b_2b_3^*)$	BR
$\check{C}_x$	$-\mathrm{Re}(H_1H_3^*+H_2H_4^*)$	$\mathrm{Im}(b_1b_4^*-b_2b_3^*)$	
$\check{C}_z$	$\frac{1}{2}(-\lvert H_1\rvert^2-\lvert H_2\rvert^2+\lvert H_3\rvert^2+\lvert H_4\rvert^2)$	$-\mathrm{Re}(b_1b_4^*+b_2b_3^*)$	
$\check{T}_x$	$\mathrm{Re}(H_1H_4^*+H_2H_3^*)$	$\mathrm{Re}(b_1b_2^*-b_3b_4^*)$	
$\check{T}_z$	$\mathrm{Re}(H_1H_2^*-H_3H_4^*)$	$\mathrm{Im}(b_1b_2^*-b_3b_4^*)$	TR
$\check{L}_x$	$-\mathrm{Re}(H_1H_3^*-H_2H_4^*)$	$\mathrm{Im}(b_1b_2^*+b_3b_4^*)$	
$\check{L}_z$	$\frac{1}{2}(\lvert H_1\rvert^2-\lvert H_2\rvert^2-\lvert H_3\rvert^2+\lvert H_4\rvert^2)$	$\mathrm{Re}(b_1b_2^*+b_3b_4^*)$	

$I=(k/q)\,d\sigma/d\Omega$ and $\check{O}=I\,O$

cross section and polarization observables

16 polarization observables in photoproduction of pseudoscalar mesons

π,η,η', K

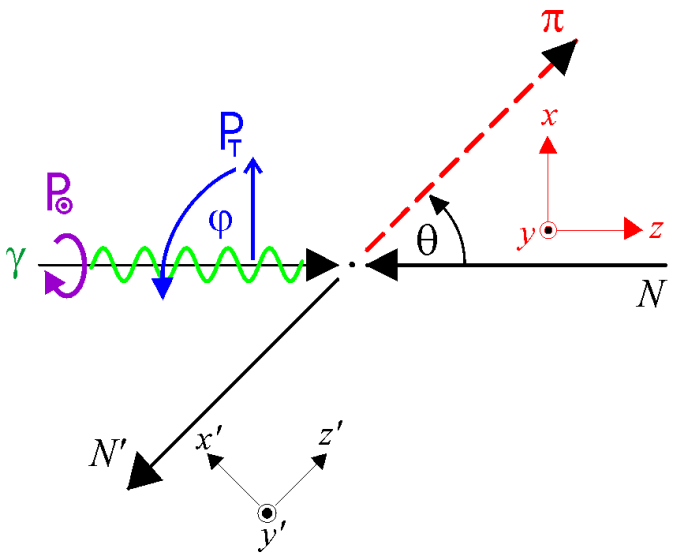

- polarized photons and polarized target

$$\frac{d\sigma}{d\Omega} = \sigma_0 \left[1 - P_T \Sigma \cos 2\varphi + P_x(-P_T H \sin 2\varphi + P_\odot F) - P_y(-T + P_T P \cos 2\varphi) - P_z(-P_T G \sin 2\varphi + P_\odot E) \right]$$

- polarized photons and recoil polarization

$$\frac{d\sigma}{d\Omega} = \sigma_0 \left[1 - P_T \Sigma \cos 2\varphi + P_{x'}(-P_T O_{x'} \sin 2\varphi - P_\odot C_{x'}) - P_{y'}(-P + P_T T \cos 2\varphi) - P_{z'}(P_T O_{z'} \sin 2\varphi + P_\odot C_{z'}) \right]$$

- polarized target and recoil polarization

$$\frac{d\sigma}{d\Omega} = \sigma_0 \left[1 + P_{y'} P + P_x(P_{x'} T_{x'} + P_{z'} T_{z'}) + P_y(T + P_{y'} \Sigma) - P_z(P_{x'} L_{x'} - P_{z'} L_{z'}) \right]$$

16 spin observables in photoproduction

linear and circular polarized beams

longitudinal and transverse polarized targets

recoil polarization, in particular for $K\Lambda$ and $K\Sigma$

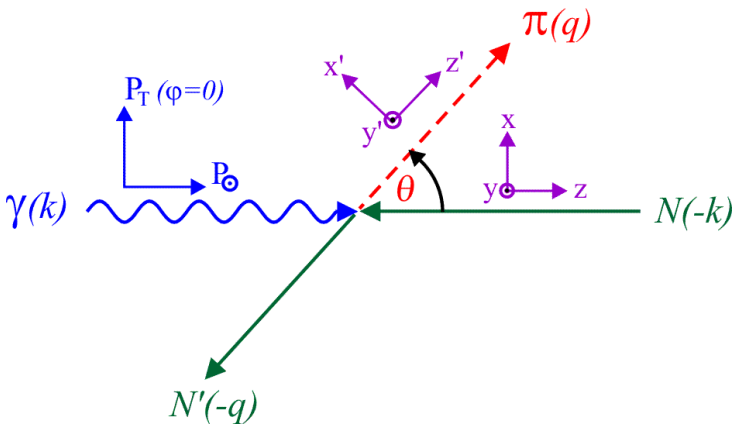

Photon		Beam - Target			Beam - Recoil			Target - Recoil			
	–	–	–	–	x'	y'	z'	x'	x'	z'	z'
	–	x	y	z	–	–	–	x	z	x	z
unpolarized	σ	0	T	0	0	P	0	$T_{x'}$	$L_{x'}$	$T_{z'}$	$L_{z'}$
linear polariz.	Σ	H	P	G	$O_{x'}$	T	$O_{z'}$	$L_{z'}$	$T_{z'}$	$L_{x'}$	$T_{x'}$
circular polariz.	0	F	0	E	$C_{x'}$	0	$C_{z'}$	0	0	0	0

8 observ. 12 observ.

16 Polarization Observables in Pion Photoproduction

in 32 different set-ups

Photon		Target			Recoil			Target – Recoil								
	–	–	–	–	x'	y'	z'	x'	x'	x'	y'	y'	y'	z'	z'	z'
	–	x	y	z	–	–	–	x	y	z	x	y	z	x	y	z
unpolarized	σ	0	T	0	0	P	0	$T_{x'}$	0	$-L_{x'}$	0	Σ	0	$T_{z'}$	0	$L_{z'}$
lin. pol. $P_T \cos 2\varphi$	$-\Sigma$	0	$-P$	0	0	$-T$	0	$-L_{z'}$	0	$T_{z'}$	0	$-\sigma$	0	$-L_{x'}$	0	$-T_{x'}$
lin. pol. $P_T \sin 2\varphi$	0	$-H$	0	G	$-O_{x'}$	0	$-O_{z'}$	0	$-C_{z'}$	0	E	0	F	0	$C_{x'}$	0
circ. pol. $P_\odot$	0	F	0	$-E$	$-C_{x'}$	0	$-C_{z'}$	0	$O_{z'}$	0	G	0	H	0	$-O_{x'}$	0

1 unpolarized observable: σ

3 single polarization observables: Σ, T, P

4 B-T double polarization observables: E, F, G, H

4 B-R double polarization observables: Ox', Oz', Cx', Cz'

4 T-R double polarization observables: Tx', Tz', Lx', Lz'

redundant observables:

3 double polarization observables: Σ, T, P

13 triple polarization observables: σ, E, F, G, H, Ox', Oz', Cx', Cz', Tx', Tz', Lx', Lz'

Complete Experiments in Pion Photoproduction

Photon		Target			Recoil			Target – Recoil								
	–	–	–	–	x'	y'	z'	x'	x'	x'	y'	y'	y'	z'	z'	z'
	–	x	y	z	–	–	–	x	y	z	x	y	z	x	y	z
unpolarized	σ	0	T	0	0	P	0	$T_{x'}$	0	$-L_{x'}$	0	Σ	0	$T_{z'}$	0	$L_{z'}$
lin. pol. $P_T \cos 2\varphi$	$-\Sigma$	0	$-P$	0	0	$-T$	0	$-L_{z'}$	0	$T_{z'}$	0	$-\sigma$	0	$-L_{x'}$	0	$-T_{x'}$
lin. pol. $P_T \sin 2\varphi$	0	$-H$	0	G	$-O_{x'}$	0	$-O_{z'}$	0	$-C_{z'}$	0	E	0	F	0	$C_{x'}$	0
circ. pol. $P_\odot$	0	F	0	$-E$	$-C_{x'}$	0	$-C_{z'}$	0	$O_{z'}$	0	G	0	H	0	$-O_{x'}$	0

For a complete experiment one needs at least 8 observables

mathematically there are $\binom{16}{8} = 12870$ possibilities, 10 030 are complete!

No set is easy to measure, all require at least 2 beam-target and 2 beam-recoil polarization observ.

If one fixes the „easy“ set of {σ, Σ, T, P}

and avoids the most difficult Target-Recoil,

there are only 20 complete sets,
some of them are:

Set	group $\mathcal{S}$				group $\mathcal{BT}$		group $\mathcal{BR}$	
1	σ	Σ	T	P	E	F	$C_{x'}$	$O_{x'}$
2	σ	Σ	T	P	E	F	$C_{z'}$	$O_{z'}$
3	σ	Σ	T	P	E	G	$C_{x'}$	$C_{z'}$
8	σ	Σ	T	P	E	G	$O_{x'}$	$O_{z'}$
9	σ	Σ	T	P	E	H	$C_{x'}$	$O_{x'}$

more on complete experiments tomorow afternoon

Models
with

Born terms

t-channel exchanges

Resonance excitations

see a very good overview with a comparison of
SAID, MAID, Bonn-Gatchina and Jülich-Bonn on:
The impact of new polarization data from Bonn, Mainz and JLab
Anisovich et al., Eur. Phys. J. A (2016) 52: 284

Dynamical coupled-channel models

The Jülich-Bonn model

e.g. Döring, Hanhart, Huang, Krewald, Meißner, Rönchen, Nucl. Phys. A851 (2011) 58

Lippmann-Schwinger equation in the partial-wave basis

$$T_{\alpha\beta}(q,p',E) = V_{\alpha\beta}(q,p',W) + \sum_{\kappa} \int_0^{\infty} dp\, p^2\, V_{\alpha\kappa}(q,p,W) G_{\kappa}(p,W)\, T_{\kappa\beta}(p,p',W)$$

$$V_{\alpha\beta} = \sum_{i=0}^{n} \frac{\gamma^{a}_{\alpha;i}\,\gamma^{c}_{\beta;i}}{W - m_i^b} + V^{\mathrm{NP}}_{\alpha\beta} + \frac{1}{m_N}\gamma^{\mathrm{CT};a}_{\alpha}\gamma^{\mathrm{CT};c}_{\beta}$$

bare resonances — background with Born terms, contact terms, etc.

$\{\alpha,\beta,\kappa\}$ are initial, final and intermediate meson-baryon channels

two-body channels: (γN), πN, ηN, $K\Lambda$, $K\Sigma$, $(\omega N, \eta\prime N)$

effective three-body channels: σN, $\pi\Delta$, ρN

resonance parameters as mass and couplings are bare parameters

the dressed resonance parameters are obtained from the solutions of the LS eq.

Unitary Isobar Model MAID

e.g. Drechsel, Kamalov, Tiator, Eur. Phys. J. A 34 (2007) 69

single-channel isobar models

in the spirit of the dynamical approach to $\{\pi,K,\eta,\eta',\pi\pi\}$ photo- and electroproduction

$$T_{\gamma\pi}(W,Q^2) = T^B_{\gamma\pi}(W,Q^2) + T^R_{\gamma\pi}(W,Q^2)$$

$$T^B_{\gamma\pi}(W,Q^2) = V^B_{\gamma\pi}(W,Q^2)\,[1 + i\,T_{\pi N}(W)]$$

$$T^R_{\gamma\pi}(W,Q^2) = \bar{\mathcal{A}}^R(W,Q^2)\,\frac{f_{\gamma N}(W)\,\Gamma_{\rm tot}(W)\,M_R\,f_{\pi N}(W)}{M_R^2 - W^2 - i\,M_R\,\Gamma_{\rm tot}(W)}\,e^{i\phi_R(W,Q^2)}$$

approximations in this approach:

- the background is treated in K-matrix approximation only with πN channel
- the PV integral contribution is neglected or partly absorbed in the resonances
- the resonance part is parameterized such that loop and cc are included effectively in terms of dressed resonances

Born terms

The Born terms can most easily be expressed in terms of invariant amplitudes:

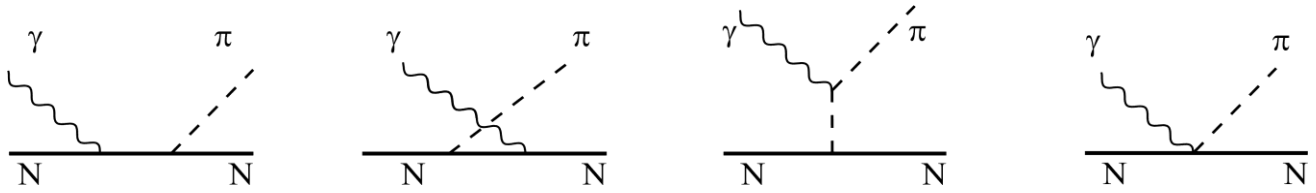

The nucleon pole contributions $A_i^{I,pole}$ $(I = 0, +, -)$ are given by

$$
\begin{aligned}
A_1^{I,pole} &= \frac{e\, g_{\pi N}}{2}\left(\frac{1}{s-M_N^2}+\frac{\varepsilon^I}{u-M_N^2}\right)\\
A_2^{I,pole} &= -\frac{e\, g_{\pi N}}{t-M_\pi^2}\left(\frac{1}{s-M_N^2}+\frac{\varepsilon^I}{u-M_N^2}\right)\\
A_3^{I,pole} &= -\frac{e\, g_{\pi N}}{2M_N}\frac{\kappa^I}{2}\left(\frac{1}{s-M_N^2}-\frac{\varepsilon^I}{u-M_N^2}\right)\\
A_4^{I,pole} &= -\frac{e\, g_{\pi N}}{2M_N}\frac{\kappa^I}{2}\left(\frac{1}{s-M_N^2}+\frac{\varepsilon^I}{u-M_N^2}\right)
\end{aligned}
$$

with $\varepsilon^+ = \varepsilon^0 = -\varepsilon^- = 1$, $\kappa^{(+,-)} = \kappa_p - \kappa_n$, and $\kappa^{(0)} = \kappa_p + \kappa_n$,
where κ_p and κ_n are the anomalous magnetic moments of the proton and the neutron

the nucleon pole contributions correspond to the Borm terms in pseudoscalar γ_5 coupling
for pseudovector $\gamma_5\,\gamma^\mu$ coupling an additional term arises for A_1
which can also be derived with dispersion relations
by the FFR sum rule (Pasquini, Drechsel, Tiator, 2007)

$$A_1^{(+,0),PV} = \frac{e\, g_{\pi N}}{2}\frac{\kappa^{(+,0)}}{2M_N^2}$$

t-channel exchanges

vector and axial vector mesons can be exchanged in the *t* channel

(here we concentrate on neutral channels as π^0,η)

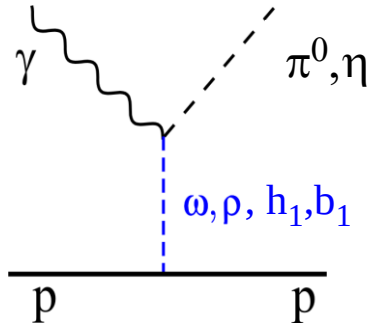

$$A_1(t) = \frac{e\lambda_V g_V^{(T)}}{2M_N M_\pi}\frac{t}{t-M_V^2}$$

$$A_2'(t) = -\frac{e\lambda_A g_A^{(T)}}{2M_N M_\pi}\frac{t}{t-M_A^2}$$

$$A_3(t) = \frac{e\lambda_A g_A^{(V)}}{M_\pi}\frac{1}{t-M_A^2}$$

$$A_4(t) = \frac{-e\lambda_V g_V^{(V)}}{M_\pi}\frac{1}{t-M_V^2}$$

by using $A_2'(t) = A_1(t) + tA_2(t)$ instead of A_2

the 4 different couplings of V and A mesons
can be separated in the 4 Invariant Amplitudes

	γ	π^0	η	$\rho(770)$	$\omega(782)$	$h_1(1120)$	$b_1(1235)$
I^G	$0,1$	1^-	0^+	1^+	0^-	0^-	1^+
J^{PC}	1^{--}	0^{-+}	0^{-+}	1^{--}	1^{--}	1^{+-}	1^{+-}

for π^0,η photoproduction *C* parity is conserved

P	J^P	coupling	IA	mesons
n	$1^-,2^+,\ldots$	$g_V^{(V)}\gamma^\mu$	A_4	ρ,ω,ϕ
n	$1^-,2^+,\ldots$	$g_V^{(T)}\sigma^{\mu\nu}$	A_1	ρ,ω,ϕ
u	$1^+,2^-,\ldots$	$g_A^{(V)}\gamma^\mu\gamma_5$	A_3	ρ_2,ω_2
u	$1^+,2^-,\ldots$	$g_A^{(T)}\sigma^{\mu\nu}\gamma_5$	A_2'	h_1,b_1

natural and un-natural parity exchanges

Reggeization of *t*-channel exchanges

see also talks by V. Matthieu, J. Nys and V. Kashevarov

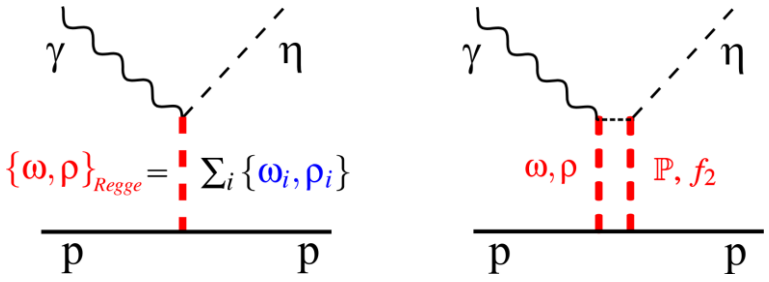

Regge Regge cuts

Regge trajectories for ω,ρ

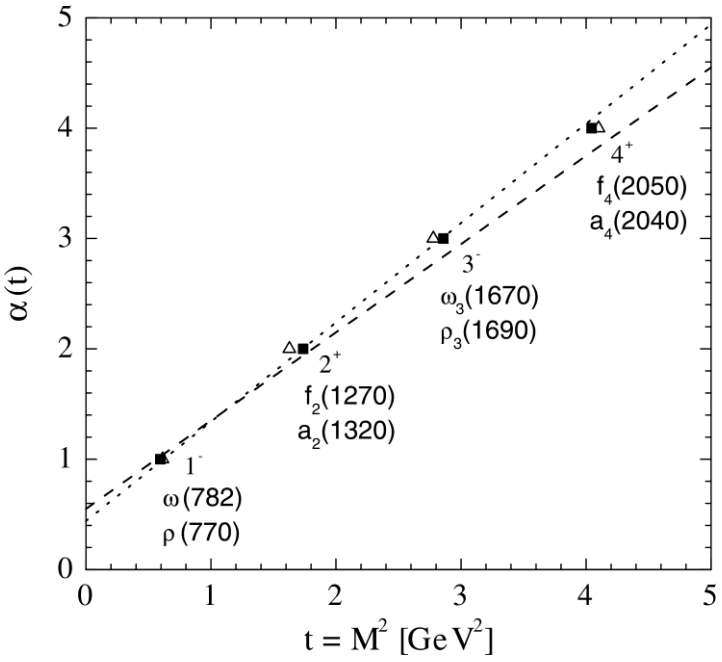

going from the pole model to the Regge model
only the propagators must be exchanged:

$$\frac{1}{t - M^2_{V,A}} \quad \Rightarrow \quad D_{V,A}$$

$$= \left(\frac{s}{s_0}\right)^{\alpha_{V,A}(t)-1} \frac{\pi\alpha'_{V,A}\left(e^{-i\pi\alpha_{V,A}(t)} - 1\right)}{2\sin[\pi\alpha_{V,A}(t)]\,\Gamma[\alpha_{V,A}(t)]}$$

alternatively, if s/s_0 is replaced by ν/ν_0
fixed-*t* dispersion relations hold for the Regge amplitudes

$$D_{V,A} = \left(\frac{\nu}{\nu_0}\right)^{\alpha_{V,A}(t)-1} \frac{\pi\alpha'_{V,A}\left(e^{-i\pi\alpha_{V,A}(t)} - 1\right)}{2\sin[\pi\alpha_{V,A}(t)]\,\Gamma[\alpha_{V,A}(t)]}$$

Regge cuts
effectively describe
the exchange of 2 trajectories
as ρ+$\mathbf{f_2}$ or ρ+$\boldsymbol{P}$ etc.
and can contribute
to all 4 inv. amplitudes

Donnachie, Kalashnikova, 2016

Resonance excitations

isospin conservation:
in πN and $K\Sigma$ N^* and Δ can be excited
in ηN, $\eta' N$ and $K\Lambda$ only N^* are possible

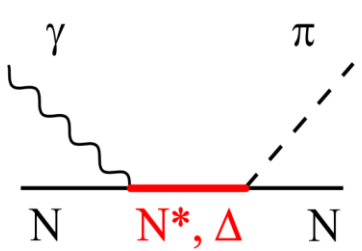

in s channel:
N*,Δ can be excited on shell

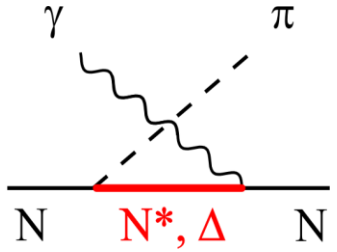

in u channel:
N*,Δ are off-shell

therefore, crossing symmetry is violated in any case
the u channel acts more like a background and can be absorbed by other bg contributions

crossing symmetry can be restored with fixed-t dispersion relations

Breit-Wigner ansatz for s-channel resonance excitations:

$$\mathcal{M}_{\ell\pm}(W) = \bar{\mathcal{M}}_{\ell\pm} f_{\gamma N}(W) \frac{M_R \Gamma_{\text{tot}}(W)}{M_R^2 - W^2 - i M_R \Gamma_{\text{tot}}(W)} f_{\pi N}(W) C_{\pi N}$$

$$f_{\pi N}(W) = \zeta_{\pi N} \left[\frac{1}{(2J+1)\pi} \frac{k}{q} \frac{M_N}{W} \frac{\Gamma_{\pi N}(W)}{\Gamma_{\text{tot}}(W)^2} \right]^{1/2}$$

$$f_{\gamma N}(W) = \left(\frac{k}{k_R} \right)^2 \left(\frac{X^2 + k_R^2}{X^2 + k^2} \right)^2$$

$C_{\pi N}$ is an isospin factor:

$$C_{\pi N} = \begin{cases} -1/\sqrt{3} & : \quad I = 1/2 \\ \sqrt{3/2} & : \quad I = 3/2 \end{cases}$$

for η and η' production:

$$C_{\eta N} = C_{\eta' N} = -1$$

$\zeta_{\pi N}$ is a relative phase
of an individual resonance:

$$\zeta_{\pi N} = 1, \; \zeta_{\eta N} = \pm 1, \; \zeta_{\eta' N} = \pm 1$$

energy-dependent width

The width of a Breit-Wigner resonance must be energy dependent.
Without the energy dependence, it is just a pole Ansatz
and works only in a narrow region around an isolated resonance, very bad for baryons.

The following Ansatz provides a correct threshold behavior.
At the resonance position $W = M_R$ it is normalized to the full width.
At high energy the Ansatz is more flexible and model dependent.

Threshold energies in MeV of various N^* decay channels

πN	$\pi\pi N$	ηN	$K\Lambda$	$K\Sigma$	ωN	$\eta' N$
1077.84	1217.41	1486.13	1609.36	1686.32	1720.92	1896.05

$$\Gamma_{\rm tot}(W) = \Gamma_{\pi N}(W) + \Gamma_{\pi\pi N}(W) + \Gamma_{\eta N}(W) + \Gamma_{K\Lambda}(W) + \cdots$$

$$\Gamma_{\pi N}(W) = \beta_{\pi N}\,\Gamma_R \left(\frac{q_\pi}{q_{\pi,R}}\right)^{2\ell+1} \left(\frac{X^2+q_{\pi,R}^2}{X^2+q_\pi^2}\right)^{\ell} \frac{M_R}{W}$$

$$\Gamma_{\eta N}(W) = \beta_{\eta N}\,\Gamma_R \left(\frac{q_\eta}{q_{\eta,R}}\right)^{2\ell+1} \left(\frac{X^2+q_{\eta,R}^2}{X^2+q_\eta^2}\right)^{\ell} \frac{M_R}{W}$$

$$\vdots$$

$$\Gamma_{\pi\pi N}(W) = (1-\beta_{\pi N}-\beta_{\eta N}-\cdots)\,\Gamma_R \left(\frac{q_{2\pi}}{q_{2\pi,R}}\right)^{2\ell+4} \left(\frac{X^2+q_{2\pi,R}^2}{X^2+q_{2\pi}^2}\right)^{\ell+2}$$

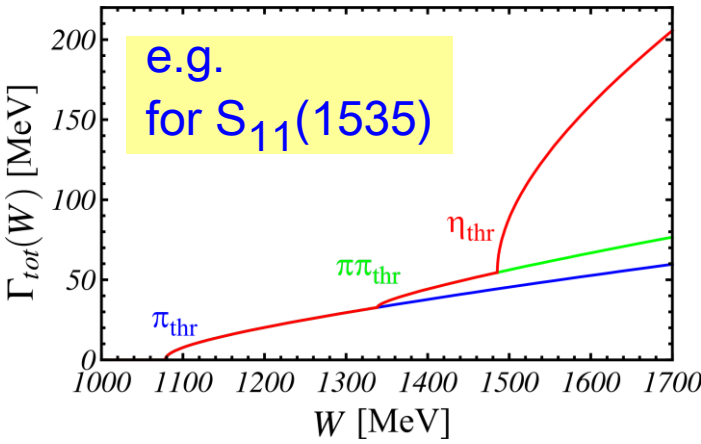

photon decay amplitudes

$$\bar{M}_{\ell+} = -\frac{1}{\ell+1}\left(A^{\ell+}_{1/2} + \sqrt{\frac{\ell+2}{\ell}}A^{\ell+}_{3/2}\right)$$

$$\bar{E}_{\ell+} = -\frac{1}{\ell+1}\left(A^{\ell+}_{1/2} - \sqrt{\frac{\ell}{\ell+2}}A^{\ell+}_{3/2}\right)$$

$$\bar{M}_{\ell+1,-} = +\frac{1}{\ell+1}\left(A^{\ell+1,-}_{1/2} - \sqrt{\frac{\ell}{\ell+2}}A^{\ell+1,-}_{3/2}\right)$$

$$\bar{E}_{\ell+1,-} = -\frac{1}{\ell+1}\left(A^{\ell+1,-}_{1/2} + \sqrt{\frac{\ell+2}{\ell}}A^{\ell+1,-}_{3/2}\right)$$

N^*,Δ	$\bar{E}$	$\bar{M}$
S_{11}, S_{31}	$-A_{1/2}$	—
P_{11}, P_{31}	—	$A_{1/2}$
P_{13}, P_{33}	$\frac{1}{2}(\frac{1}{\sqrt{3}}A_{3/2} - A_{1/2})$	$-\frac{1}{2}(\sqrt{3}A_{3/2} + A_{1/2})$
D_{13}, D_{33}	$-\frac{1}{2}(\sqrt{3}A_{3/2} + A_{1/2})$	$-\frac{1}{2}(\frac{1}{\sqrt{3}}A_{3/2} - A_{1/2})$
D_{15}, D_{35}	$\frac{1}{3}(\frac{1}{\sqrt{2}}A_{3/2} - A_{1/2})$	$-\frac{1}{3}(\sqrt{2}A_{3/2} + A_{1/2})$
F_{15}, F_{35}	$-\frac{1}{3}(\sqrt{2}A_{3/2} + A_{1/2})$	$-\frac{1}{3}(\frac{1}{\sqrt{2}}A_{3/2} - A_{1/2})$

the advantage of such a Breit-Wigner Ansatz is that most parameters are observable quantities and are listed in the Particle Data Tables:

M_R : mass

Γ_R : width

β_i : branching ratios

$A_{1/2}$, $A_{3/2}$: photon decay amplitudes

However, the whole Ansatz is model dependent by itself
For strong and non-overlapping resonances the model dependence is weak
For overlapping and broad resonances the model dependence can be very large

MAID2007 with only 4-star resonances in γ,π

PDG 2016 N* resonance table

7 N**** in MAID2007

Particle	J^P	overall	$N\gamma$	$N\pi$	$N\eta$	$N\sigma$	$N\omega$	ΛK	ΣK	$N\rho$	$\Delta\pi$
N	$1/2^+$	****									
$N(1440)$	$1/2^+$	****	****	****		***				*	***
$N(1520)$	$3/2^-$	****	****	****	***					***	***
$N(1535)$	$1/2^-$	****	****	****	****					**	*
$N(1650)$	$1/2^-$	****	***	****	***			***	**	**	***
$N(1675)$	$5/2^-$	****	***	****	*			*		*	***
$N(1680)$	$5/2^+$	****	****	****	*	**				***	***
$N(1700)$	$3/2^-$	***	**	***	*			*	*	*	***
$N(1710)$	$1/2^+$	****	****	****	***		**	****	**	*	**
$N(1720)$	$3/2^+$	****	***	****	***			**	**	**	*
$N(1860)$	$5/2^+$	**		**						*	*
$N(1875)$	$3/2^-$	***	***	*			**	***	**		***
$N(1880)$	$1/2^+$	**	*	*		**		*			
$N(1895)$	$1/2^-$	**	**	*	**			**	*		
$N(1900)$	$3/2^+$	***	***	**	**		**	***	**	*	**
$N(1990)$	$7/2^+$	**	**	**					*		

MAID2007 with only 4-star resonances in γ,π

PDG 2016 N* resonance table

6 Δ**** in MAID2007

Particle	J^P	overall	$N\gamma$	$N\pi$	$N\eta$	$N\sigma$	$N\omega$	ΛK	ΣK	$N\rho$	$\Delta\pi$
$\Delta(1232)$	$3/2^+$	****	****	****	F						
$\Delta(1600)$	$3/2^+$	***	***	***	o					*	***
$\Delta(1620)$	$1/2^-$	****	***	****		r				***	***
$\Delta(1700)$	$3/2^-$	****	****	****			b			**	***
$\Delta(1750)$	$1/2^+$	*		*				i			
$\Delta(1900)$	$1/2^-$	**	**	**					d	**	**
$\Delta(1905)$	$5/2^+$	****	****	****						***	**
$\Delta(1910)$	$1/2^+$	****	**	****						*	**
$\Delta(1920)$	$3/2^+$	***	**	***						***	**
$\Delta(1930)$	$5/2^-$	***		***							
$\Delta(1940)$	$3/2^-$	**	**	*	F						
$\Delta(1950)$	$7/2^+$	****	****	****						*	***

Eta-MAID update with new resonances

Particle	J^P	overall	$N\gamma$	$N\pi$	$N\eta$	$N\sigma$	$N\omega$	ΛK	ΣK	$N\rho$	$\Delta\pi$
N	$1/2^+$	****									
$N(1440)$	$1/2^+$	****	****	****		***				*	***
$N(1520)$	$3/2^-$	****	****	****	***					***	***
$N(1535)$	$1/2^-$	****	****	****	****					**	*
$N(1650)$	$1/2^-$	****	***	****	***			***	**	**	***
$N(1675)$	$5/2^-$	****	***	****	*			*		*	***
$N(1680)$	$5/2^+$	****	****	****	*	**				***	***
$N(1700)$	$3/2^-$	***	**	***	*			*	*	*	***
$N(1710)$	$1/2^+$	****	****	****	***		**	****	**	*	**
$N(1720)$	$3/2^+$	****	***	****	***			**	**	**	*
$N(1860)$	$5/2^+$	**		**						*	*
$N(1875)$	$3/2^-$	***	***	*			**	***	**		***
$N(1880)$	$1/2^+$	**	*	*		**		*			
$N(1895)$	$1/2^-$	**	**	*	**			**	*		
$N(1900)$	$3/2^+$	***	***	**	**		**	***	**	*	**
$N(1990)$	$7/2^+$	**	**	**					*		
$N(2000)$	$5/2^+$	**	**	*	**			**	*	**	
$N(2040)$	$3/2^+$	*		*							
$N(2060)$	$5/2^-$	**	**	**	*				**		
$N(2100)$	$1/2^+$	*		*							
$N(2120)$	$3/2^-$	**	*	**				*	*		
$N(2190)$	$7/2^-$	****	***	****			*	**		*	
$N(2220)$	$9/2^+$	****		****							
$N(2250)$	$9/2^-$	****		****							
$N(2300)$	$1/2^+$	**		**							
$N(2570)$	$5/2^-$	**		**							
$N(2600)$	$11/2^-$	***		***							
$N(2700)$	$13/2^+$	**		**							

PDG 2016 N* resonance table

8 N* in 2001/2003

14 N* new in 2015/16/17

see talk of V. Kashevarov

individual Resonance contributions to total cross sections in γ,η

example from a recent EtaMAID fit with 18 N* resonances

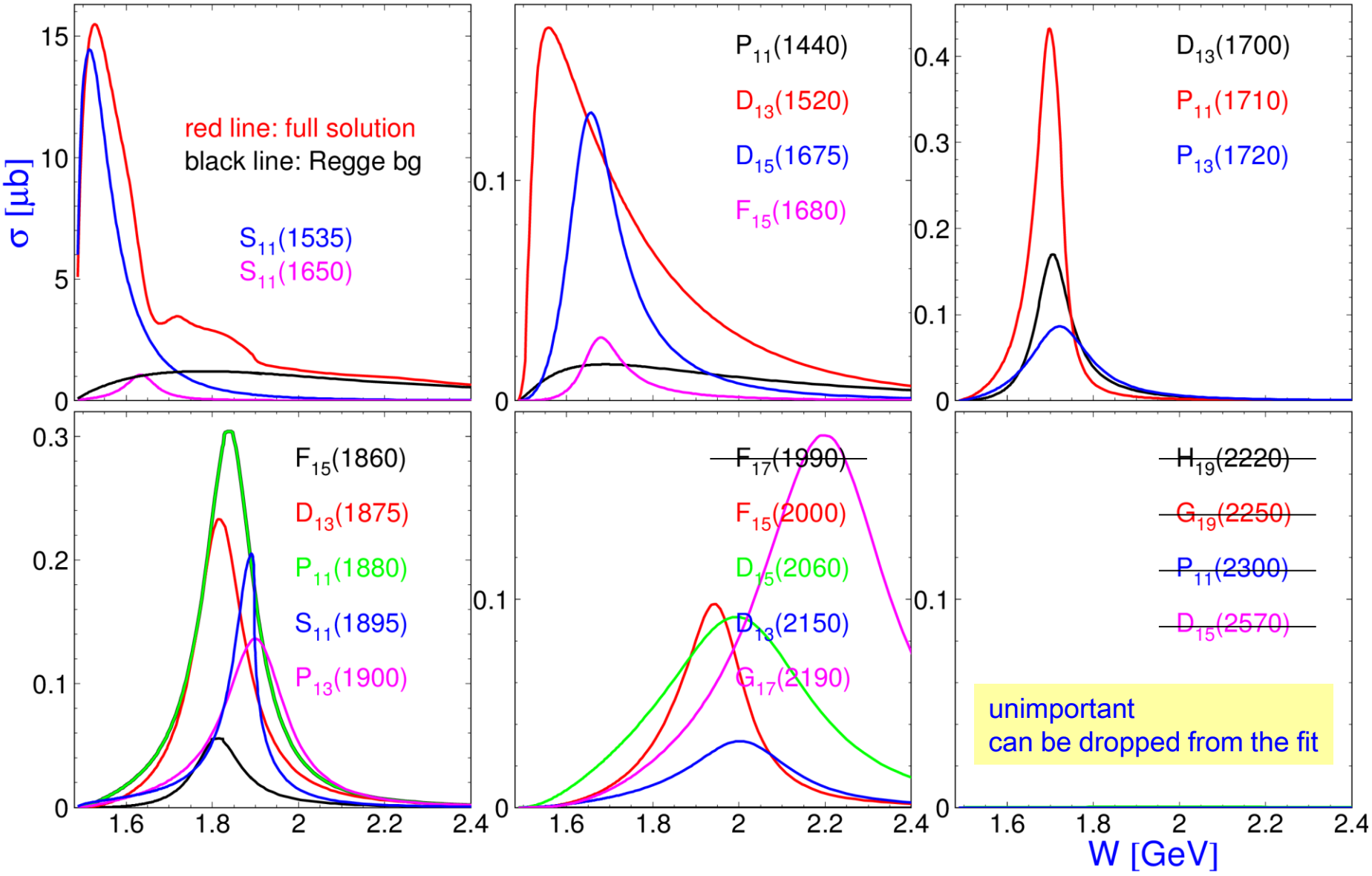

properties of baryon resonances

fundamental properties:

- pole position
- elastic residue
- inelastic residues for all decay channels

related properties:

- pole mass and pole width
- pole branching ratios for all decay channels
- photon decay amplitudes at the pole

model-dependent properties:

- Breit-Wigner mass and width
- BW branching ratios
- BW photon decay amplitudes

Residues

Branching Ratios

Photon Decay Amplitudes

Residues

Different to the mathematical definition, in particle physics, the residue is defined with an extra minus sign. In the vicinity of a pole, a T-matrix amplitude can be written as

$$T(W) \;=\; \frac{r_p}{M_p - W - \frac{i}{2}\Gamma_p} \;+\; T^{\mathrm{reg}}(W)$$

with the pole position $W_p = M_p - i\Gamma_p/2$, the residue r_p and a regular function $T^{\mathrm{reg}}(W)$. Starting with the non-relativistic form of a Breit-Wigner amplitude

$$T_{ab}(W) \;=\; \frac{\sqrt{\Gamma_a(W)/2}\,\sqrt{\Gamma_b(W)}/2}{M_{\mathrm{BW}} - W - i\Gamma_{tot}(W)/2}\,,$$

the residues of the transition amplitudes can be calculated by direct analytical continuation of the Breit-Wigner ansatz into the lower half-plane of the complex W plane.

$$Res(a \to b) \;=\; \frac{M_{\mathrm{BW}}\,\sqrt{\Gamma_a(W_p)}\,\sqrt{\Gamma_b(W_p)}}{2W_p + iM_{\mathrm{BW}}\,\Gamma'_{tot}(W_p)}\,,$$

for elastic scattering, e.g. for $\pi N \to N\pi$, this gives the elastic residue:

$$\mathrm{Res}(\pi N \to N\pi) \;=\; \frac{M_{\mathrm{BW}}\,\Gamma_{\pi N}(W_p)}{2W_p + iM_{\mathrm{BW}}\,\Gamma'_{tot}(W_p)}\,.$$

Branching ratios at the pole

In the Review of Particle Physics (PDG) normalized residues are defined as

$$\mathrm{NR}(a \to b) = \frac{Res(a \to b)}{\Gamma_p/2}\,.$$

Branching ratios at the pole can be defined by the normalized elastic residues

$$\mathrm{BR}^{pole}(b) = \frac{|Res(b \to b)|}{\Gamma_p/2}\,,$$

which can be expressed in elastic and inelastic residues due to the factorization property of residues

$$\mathrm{BR}^{pole}(b) = \frac{|Res(\pi N \to b)|^2}{|Res(\pi N \to N\pi)|\,(\Gamma_p/2)}$$

or in connection with photoproduction

$$\mathrm{BR}^{pole}(b) = \frac{|Res(\gamma N \to b)|^2}{|Res(\gamma N \to N\gamma)|\,(\Gamma_p/2)}\,.$$

Branching ratios from photoproduction

However, the elastic residues of $\gamma N \to N\gamma$ may not directly be obtained, therefore, pion photoproduction will be the ideal reaction to obtain them by

$$|Res(\gamma N \to N\gamma)| = \frac{|Res(\gamma N \to N\pi)|^2}{|Res(\pi N \to N\pi)|}\,.$$

In practise this means that the branching ratios at the pole are obtained in the following way:

- First the elastic residues $Res_{\pi N}$ will be determined from πN partial waves, and also $\mathrm{BR}_{\pi N}$.
- Second from pion photoproduction multipoles, the inelastic residues $Res_{\gamma,\pi}$ are determined and together with $Res_{\pi N}$ the elastic residues $Res_{\gamma N}$ and also $\mathrm{BR}_{\gamma N}$.
- Finally, for any other channel b, e.g. ηN, the photoproduction residues can be determined from the $E_{\ell\pm}, M_{\ell\pm}$ multipoles and together with $Res_{\gamma N}$ also the branching ratio BR_b.

Photon decay amplitudes $A_{1/2}$, $A_{3/2}$ at the pole

Workman, Tiator, Sarantsev, Phys, Rev. C87, 068201 (2013) and also PDG session, Thursday

For photoproduction, the unitary amplitude is related to the helicity amplitudes by

$$T^h_{\gamma,\pi} = \sqrt{2kq}\,\mathcal{A}^h_\alpha\, C\,,$$

with q and k being the center-of-mass pion and photon momenta. The factor C is $\sqrt{2/3}$ for isospin $3/2$ and $-\sqrt{3}$ for isospin $1/2$. For eta or etaprime photoproduction, $C = -1$.

The photon decay amplitudes $A_{1/2}$, and $A_{3/2}$ are defined at the Breit-Wigner position by

$$A^{BW}_h = C\sqrt{\frac{q_r}{k_r}\frac{\pi(2J+1)M_r\Gamma_r^2}{M_N\Gamma_{\pi,r}}}\;\tilde{\mathcal{A}}^h_\alpha\,,$$

where all quantities labeled with r are evaluated at the Breit-Wigner position $W = W_r = M_{\rm BW}$.

Similarly at the pole position we get

$$\begin{aligned} A^{pole}_h &= C\sqrt{\frac{q_p}{k_p}\frac{2\pi(2J+1)W_p}{M_N \mathrm{Res}(\pi N \to N\pi)}}\,\mathrm{Res}\,\mathcal{A}^h_\alpha \\ &= \sqrt{\frac{\pi(2J+1)W_p}{M_N k_p}}\,\frac{\mathrm{Res}(\gamma N \to b)}{\sqrt{\mathrm{Res}(b\to b)}}\,. \end{aligned}$$

Pole Positions and Residues

how can we find
the Baryon resonances
in the partial wave amplitudes

Breit-Wigner and pole position for Δ(1232)

the most important part of a dynamical model is the self-energy, arising from loop integrals of various decay channels

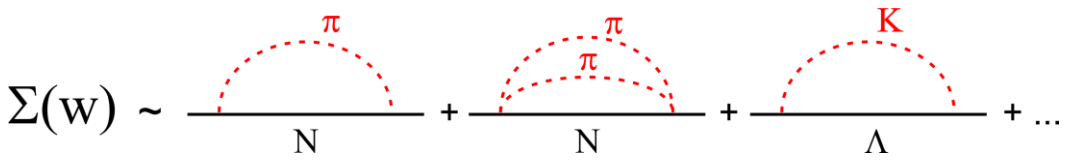

$$T(W) \sim \frac{1}{m_0 - W - \Sigma(W)} = \frac{1}{m_0 - \mathrm{Re}\,\Sigma(W) - W - i\,\mathrm{Im}\,\Sigma(W)}$$
$$\sim \frac{1}{M - W - i\Gamma(W)/2}$$

M : BW mass, $\Gamma = \Gamma(M)$: BW width

typical BW parametrization: $\Gamma(W) = \Gamma \left(\frac{q_\pi(W)}{q_\pi(M)}\right)^{2\ell+1} \left(\frac{\Lambda^2 + q_\pi(M)^2}{\Lambda^2 + q_\pi(W)^2}\right)^{\ell}$

pole position: $M - W - i\Gamma(W)/2 = 0$

solve with Mathematica FindRoot[...] or expand Γ(W) around M

for $\Delta(1232)$ resonance: $M = 1232$ MeV, $\Gamma = 115$ MeV, $\ell = 1$, $\Lambda \sim 200$ MeV

pole position: $W_{pole} = (1210 - i48)$ MeV Residue: $R_\pi = 48\, e^{-i48^\circ}$ MeV

PDG: $M = 1232$ MeV, $\Gamma = 117$ MeV, $W_{pole} = (1210 - i50)$ MeV, $R_\pi = 50\, e^{-i47^\circ}$ MeV

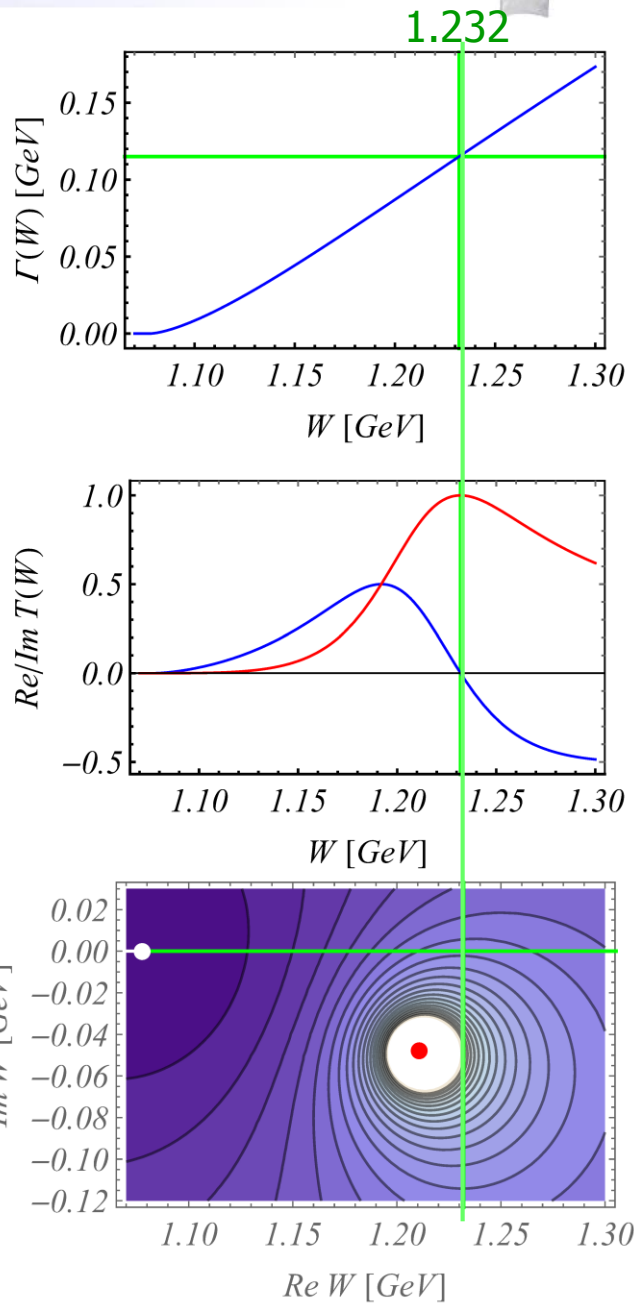

Methods for resonance analysis

old (model-dependent) Breit-Wigner analysis:

- Argan diagrams
- Breit-Wigner Ansätze

new (model-independent) pole analysis:

- Speed-Plot and Time-Delay
- Regularization method
- Padé approximation method
- Laurent plus Pietarinen (L+P) method
- Analytical Continuation

Speed-Plot and Time-Delay

summarized in sect II of: Tiator et al (Mainz-Dubna-Taipei collaboration), PR C82, 055203 (2010) with applications of πN scattering in the DMT dynamical model

The idea of the time-delay is a resonance as a quasi-stationary state with a delayed time in the scattering process. It was introduced by Eisenbud in 1948

$$\Delta t(W) = \mathrm{Re}\left(-i\frac{1}{S(W)}\frac{dS(W)}{dW}\right) = 2\frac{d\delta(W)}{dW}$$

The idea of the speed-plot is a rapid change of the scattering phase as function of energy. It was realized by the Particle Data Group already in 1971 to be a convenient tool to determine resonance poles. In 1992/93 Höhler published pole positions with the speed-plot technique for a large group of N and Δ resonances, see Particle Data Tables.

$$\mathrm{SP(W)} = \left|\frac{\mathrm{dT(W)}}{\mathrm{dW}}\right|$$

$$T(W) = \frac{r_p}{M_p - W - \frac{i}{2}\Gamma_p} + T^{\mathrm{reg}}(W)$$

if all higher order corrections are neglected, i.e. $T^{reg} = const$

$$\mathrm{SP(W)} = \frac{|\mathrm{r_p}|}{(\mathrm{W}-\mathrm{M_p})^2 + \frac{1}{4}\Gamma_\mathrm{p}^2}$$

Mp is the position of the maximum of the speed

Γp is the half-width

$$\mathrm{SP}(\mathrm{M_p} \pm \tfrac{1}{2}\Gamma_\mathrm{p}) = \tfrac{1}{2}\,\mathrm{SP}(\mathrm{M_p})$$

rp is obtained from the maximum SP(Mp)

θp is the argument ofthe complex value:

$$\theta_p = \arg\left(-\frac{dT}{dW}\bigg|_{W=M_p}\right)$$

in a single-channel analysis, the speed and the time-delay are equivalent: $\Delta t(W) = 2\,SP(W)$

Regularization Method

The idea of the speed was extended by the Zagreb group of Svarc and Ceci in 2008 by the Regularization method, which takes higher derivatives of T(W), enhancing the argument to get rid of the background.

$$T(z) = \underbrace{\frac{r}{\mu - z}}_{\text{resonant part}} + \underbrace{\left(T(z) - \frac{r}{\mu - z}\right)}_{\text{smooth background}}$$

$f(z) = (\mu - z)\,T(z)$ regular function, which can be expanded in a Taylor series around the pole, we take the N[th] derivative

pole parameters of N[th] order are obtained from a fit of a quadratic function to the N[th] order derivative of the T matrix:

$$\frac{(a_N - x)^2 + b_N^2}{\sqrt[N+1]{|r_N|^2}} = \sqrt[N+1]{\frac{(N!)^2}{\left|T^{(N)}(x)\right|^2}}$$

for a better visualization, we plot the inverse function as a speed-plot of order N

$$SP^{(N)}(W) = \sqrt[N+1]{\frac{\left|T^{(N)}(x)\right|^2}{(N!)^2}}$$

$N = 0$: $|T(W)|^2$ partial cross section

$N = 1$: $SP(W)$ normal speed-plot

$N \geq 2$: higher order derivatives of $T(W)$

Regularization Method for S_{11} with N = 0, 1, 2, 5

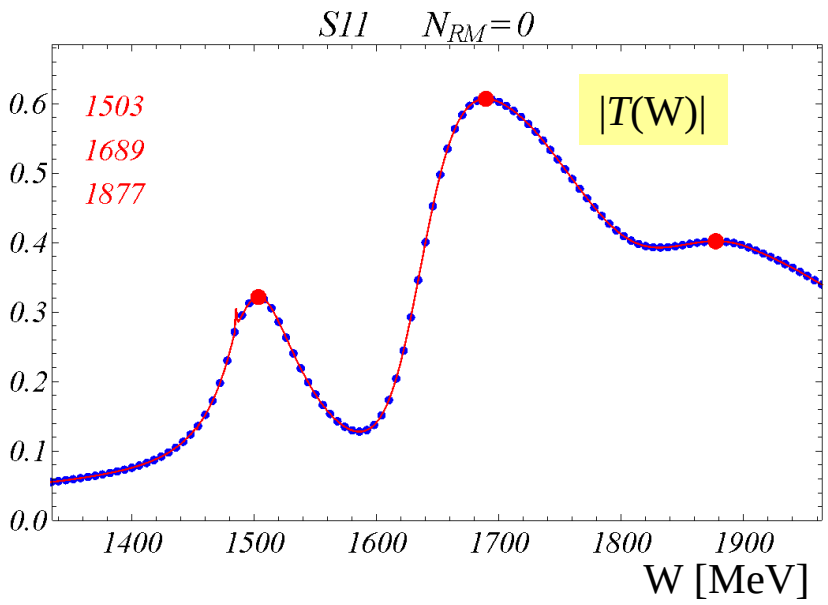

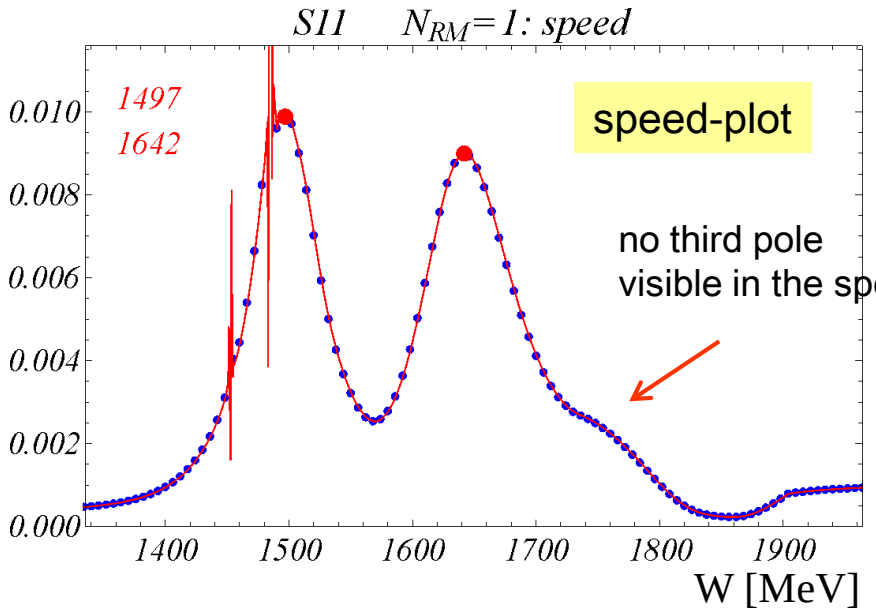

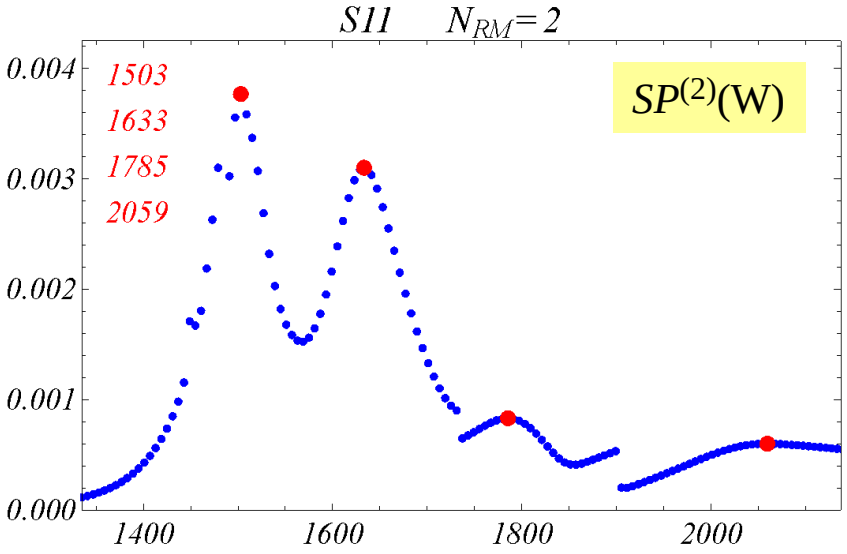

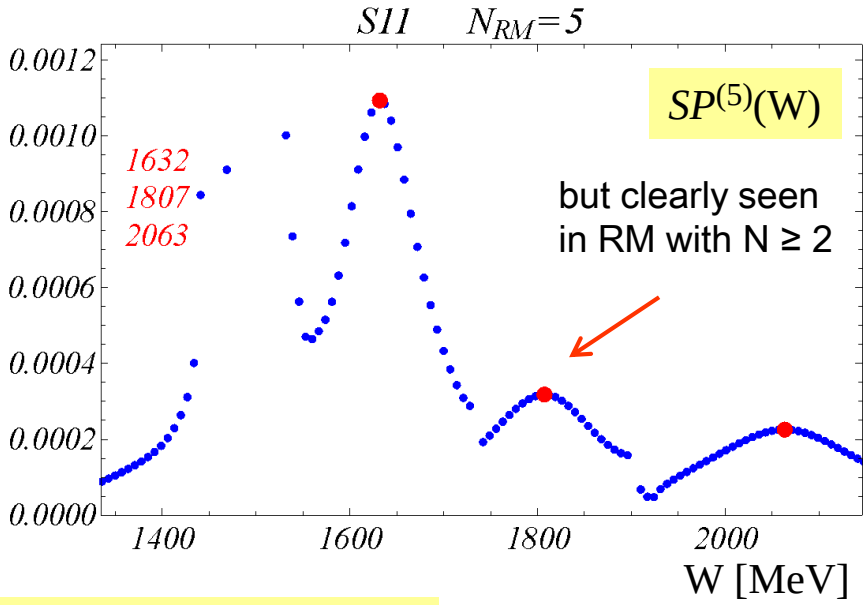

πN partial wave amplitudes from DMT model, Chen et al, PR C76, 035206 (2007)

Regularization Method for P_{11} with N = 0, 1, 2, 3

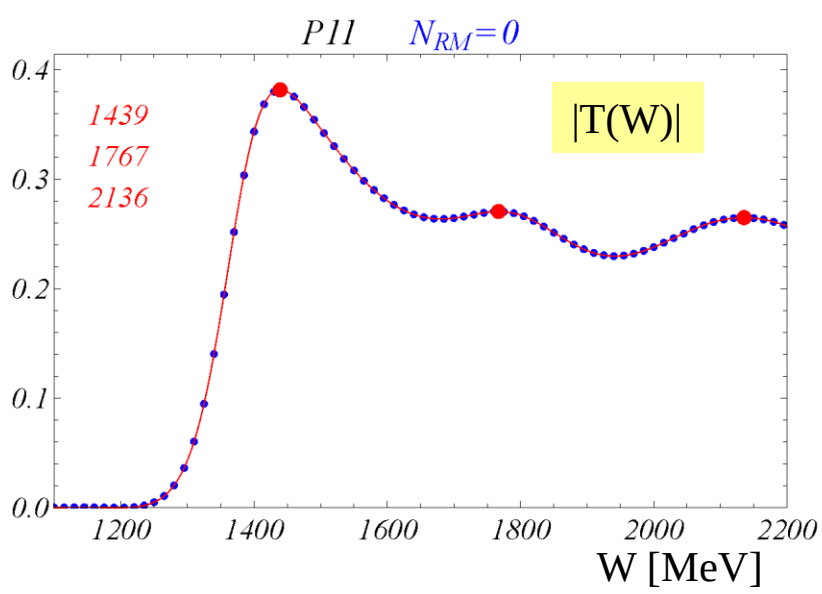

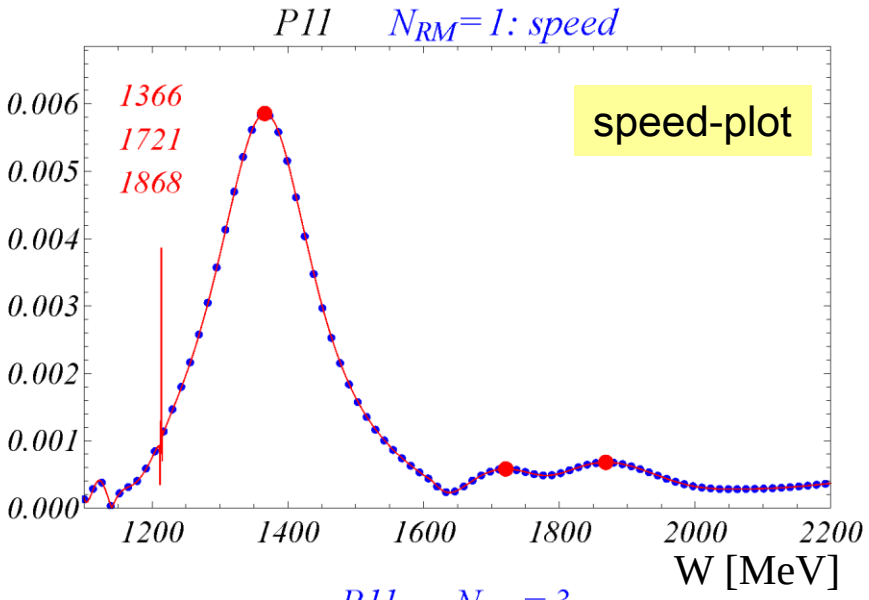

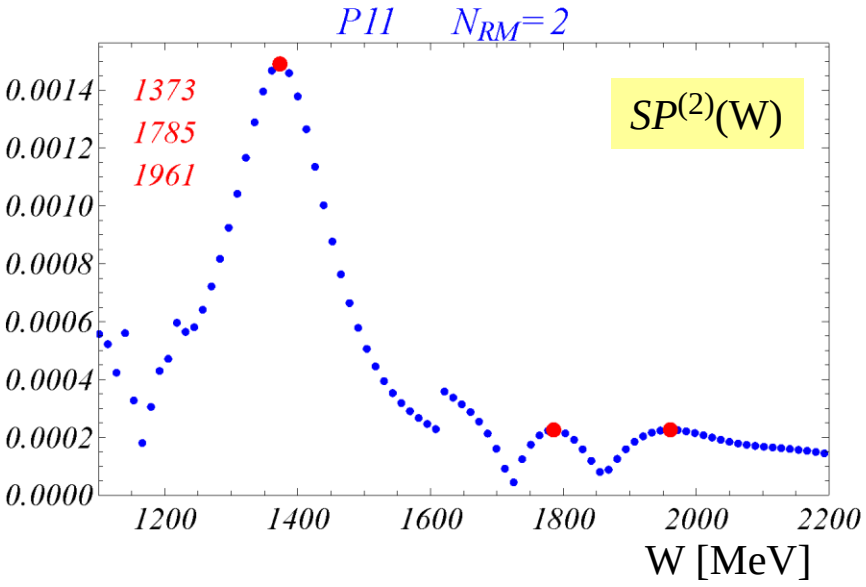

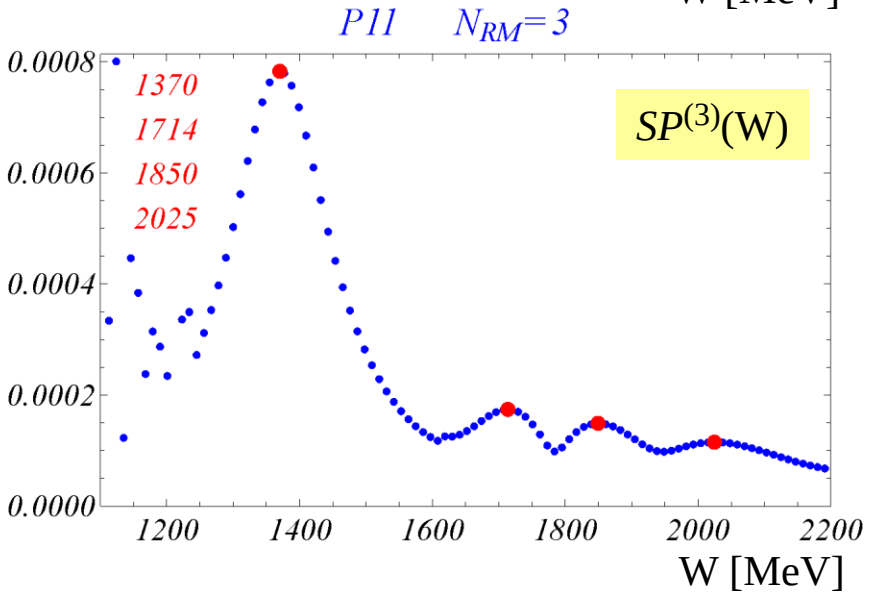

πN partial wave amplitudes from DMT model, Chen et al, PR C76, 035206 (2007)

Padé approximation method (PA)

Another very interesting method is the determination of resonance pole parameters through Padé approximants, developed by
Masjuan, Ruiz de Elvira and Sanz-Cillero, Phys. Rev. D90, 097901 (2014).

Montessus de Ballore (1902) :

If an amplitude $F(s)$ is analytic inside the disk $B_\delta(s_0)$, except for a single pole at $s = s_p$, the sequence of one-pole Padé approximants $P_1^N(s, s_0)$,

$$P_1^N(s,s_0) = \sum_{k=0}^{N-1} a_k (s-s_0)^k + \frac{a_N (s-s_0)^N}{1 - \frac{a_{N+1}}{a_N}(s-s_0)}$$

converges to $F(s)$ in any compact subset of the disk excluding the pole s_p.

Likewise, the pole and residue of the Padé approximants

$$s_p^{(N)} = s_0 + \frac{a_N}{a_{N+1}}, \qquad Z^{(N)} = -\frac{(a_N)^{N+2}}{(a_{N+1})^{N+1}}$$

converge to the corresponding pole and residue of $F(s)$ for $N \to \infty$.

PA method applied to the P_{33} pw of Maid2007

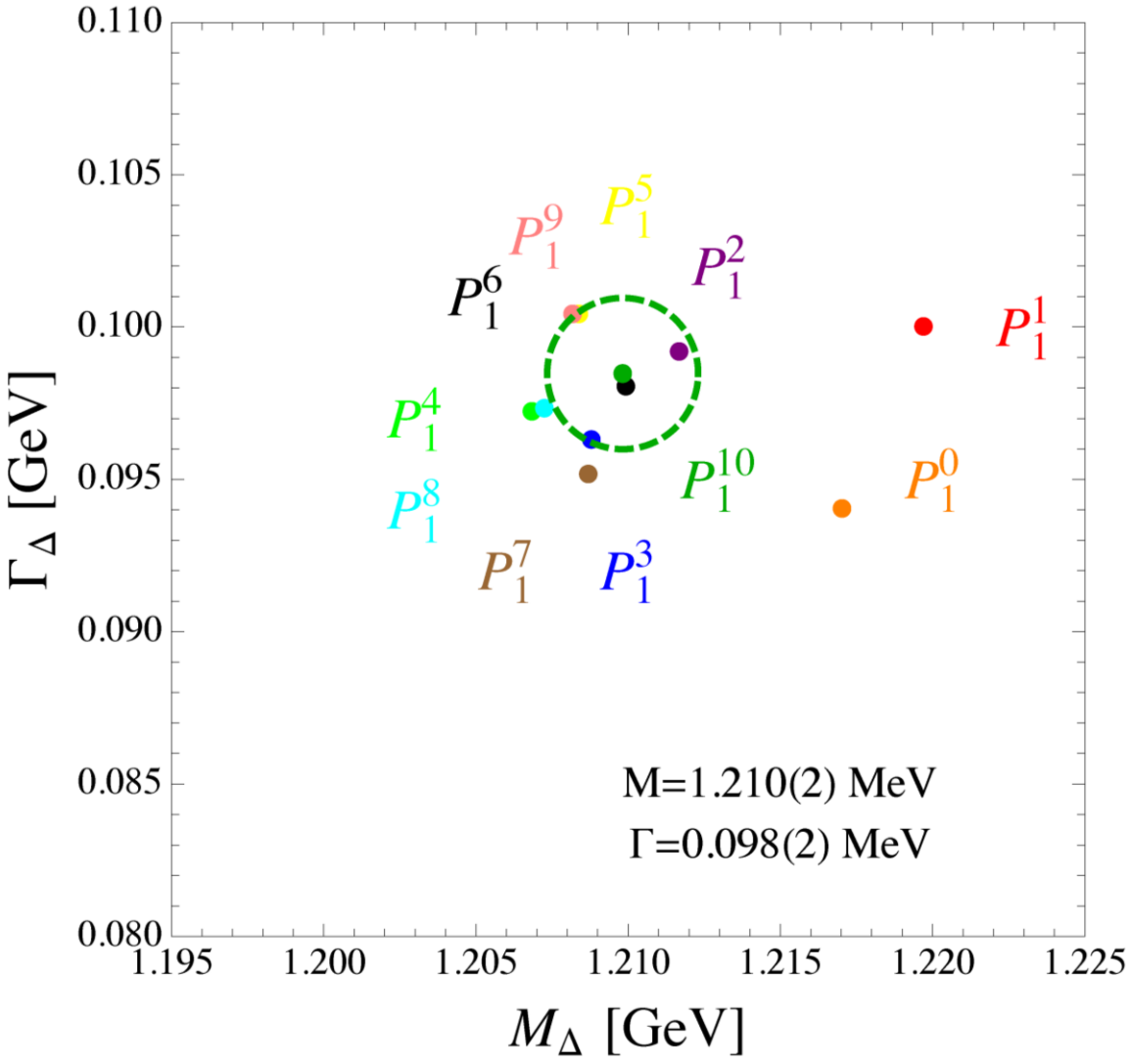

Laurent plus Pietarinen expansion (L+P)

pioneered by Alfred Svarc, Jugoslav Stahov and Zagreb/Tuzla group, 2012-2015,
e.g. Svarc, Hadzimehmedovic, Osmanovic, Stahov, Tiator, Workman, PR C88, 035206 (2013)

The L+P method defined as:

$$T(W) = \sum_{i=1}^{k} \frac{a_{-1}^{(i)}}{W - W_i} + B(W)$$

$$B(W) = \sum_{n=0}^{N_1} c_n X(W)^n + \sum_{n=0}^{N_2} d_n Y(W)^n + \sum_{n=0}^{N_3} e_n Z(W)^n + \cdots$$

$$X(W) = \frac{\alpha - \sqrt{x_P - W}}{\alpha + \sqrt{x_P - W}}; \quad Y(W) = \frac{\beta - \sqrt{x_Q - W}}{\beta + \sqrt{x_Q - W}}; \quad Z(W) = \frac{\gamma - \sqrt{x_R - W}}{\gamma + \sqrt{x_R - W}} + \cdots$$

$a_{-1}^{(i)}, W_i, W$	are complex
x_P, x_Q, x_R	are real or complex
$c_n, d_n, e_n, \alpha, \beta, \gamma$	are real

$X(W)$, $Y(W)$, $Z(W)$ make a conformal mapping of the real axis onto the unit circle
and maps the lower half-plane of the 2. Riemann sheet on to the interior of the unit circle

unlike all other methods, which act in a local area around the resonance position,
the L+P method is a global method, which describes the partial waves over the whole energy range
and is not affected by numerical problems from higher-order derivatives

Branch-points and branch-cuts

the L+P method takes the most important branch-points into account, which is a very important detail of any partial wave analysis

branch-cuts of the Jülich-Bonn model:

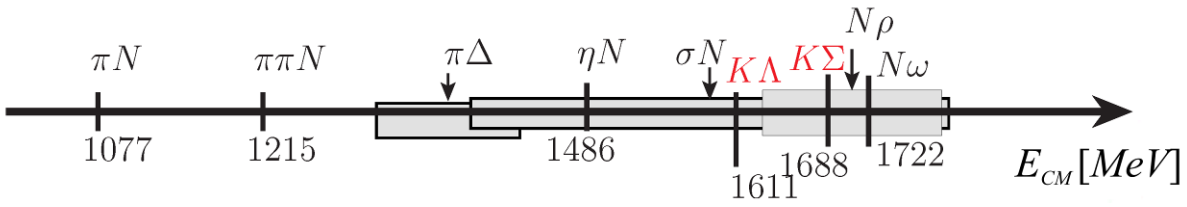

branch-points of the Jülich-Bonn model in the P_{11} channel:

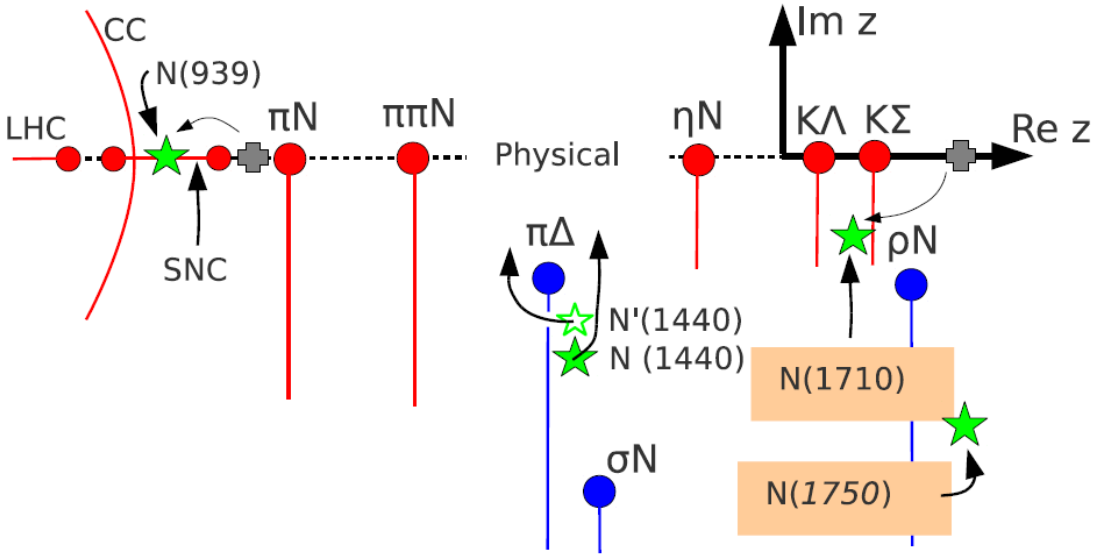

Domain of convergence of Laurent series for P_{11} partial wave

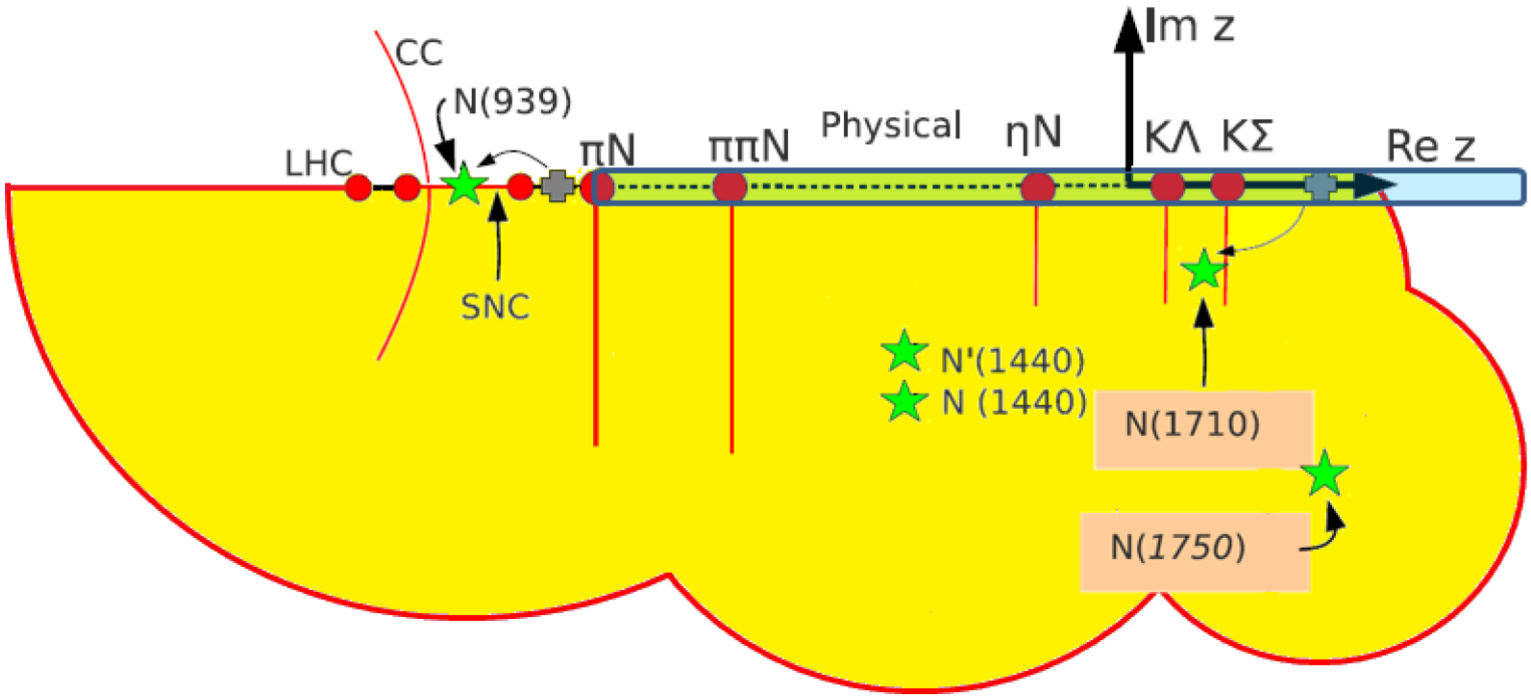

Analytical continuation (AC)

If a numerical model allows a calculation for complex energies and is continous and analytical in the region from the real (physical) axis down in the lower half-plane of the nearest Riemann sheet, then an analytical continuation would give the most accurate determination of the pole positions and the residues. (unfortunately, often not the case!)

Then the pole can be found with standard root finding procedures

from the inverted T-matrix amplitude:

$$h(z_p) = \frac{1}{|T(z_p)|} = 0$$

And the residue is found either by contour integration,

or even simpler by approaching the pole from different directions:

$$\mathrm{Res}\, T(z)\big|_{z_p} = \lim_{z \to z_p} (z - z_p)\, T(z)$$

The residues from different directions must coincide. This gives another confirmation of a first order pole position.

L+P expansion of energy-dep. (ED) solutions of DMT model

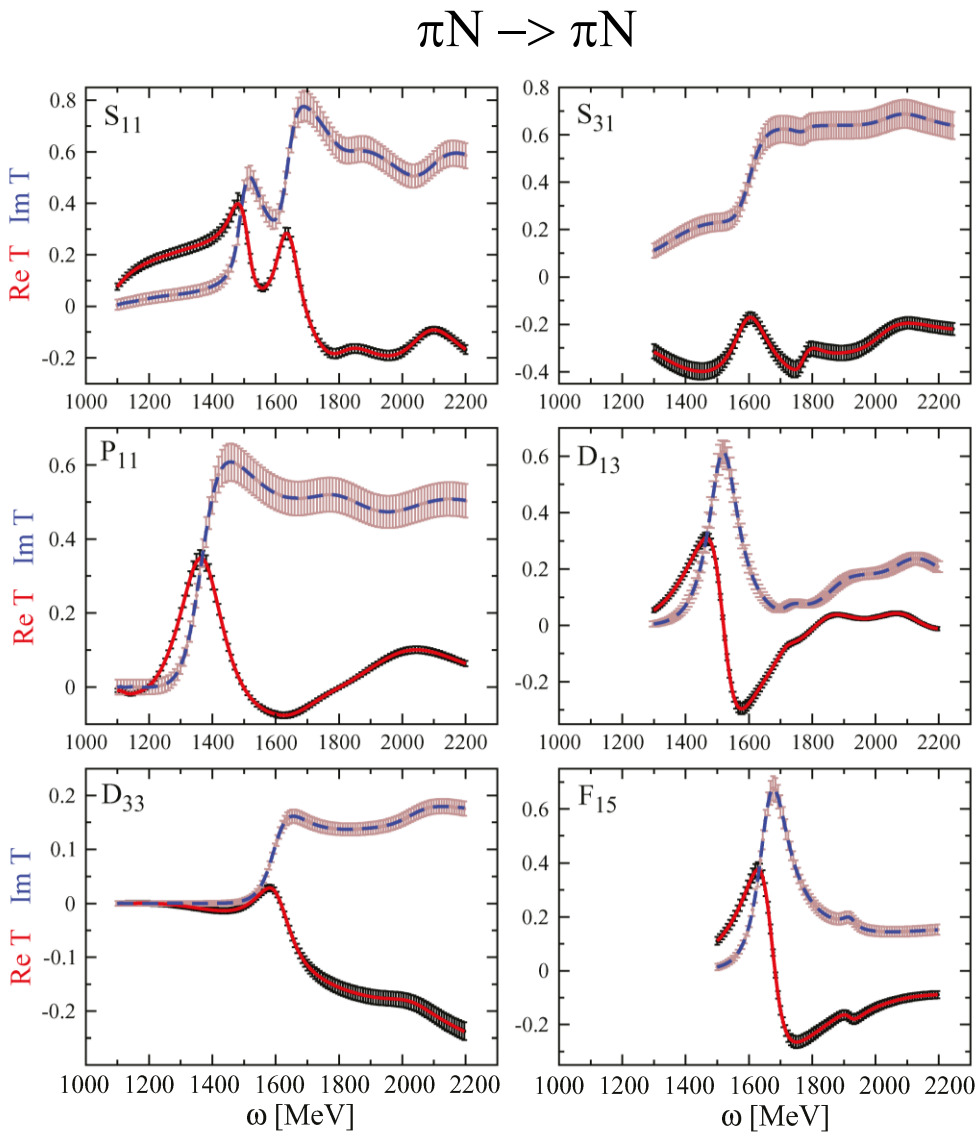

	SP	RM (N)	L+P	**AC**
1. P_{11}	1366 180 48	1371 (5) 190 50	1370 190 50	**1371** **190** **50**
2. P_{11}	1721 184 5	1756 (6) 300 11	1763 235 5	**1746** **368** **11**
1. S_{11}	1499 52 7	1499 (1) 52 7	1500 76 13.4	**1499** **78** **14**
2. S_{11}	1642 98 22	1631 (6) 104 28	1636 99 22	**1631** **120** **35**
3. S_{11}	--- -- -	1806 (6) 166 10	1810 164 10	**1733** **180** **16**

contour plot of the S11 partial wave of the DMT model

in the lower half-plane of the 2. RS

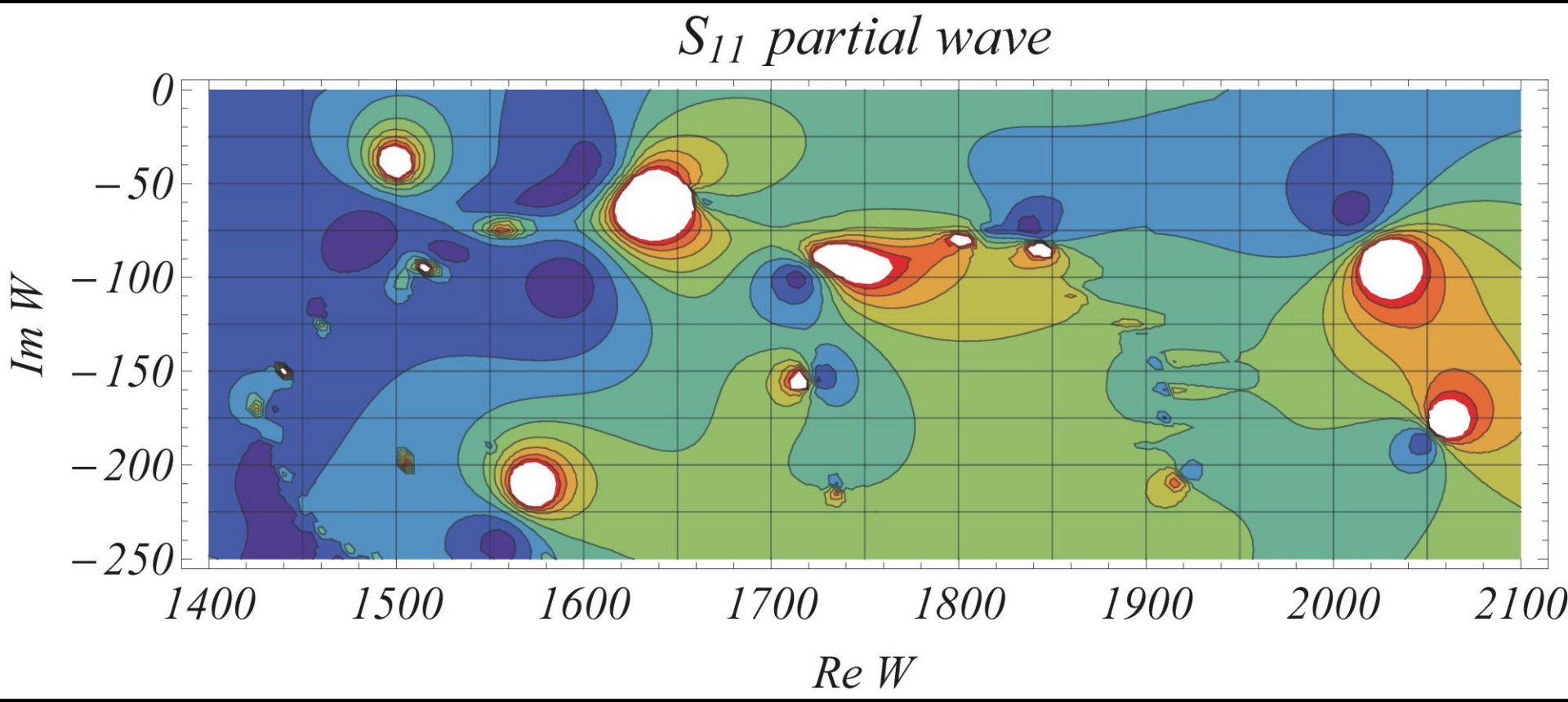

contour plot of the D13 partial wave of the DMT model in the glued first and second Riemann Sheets

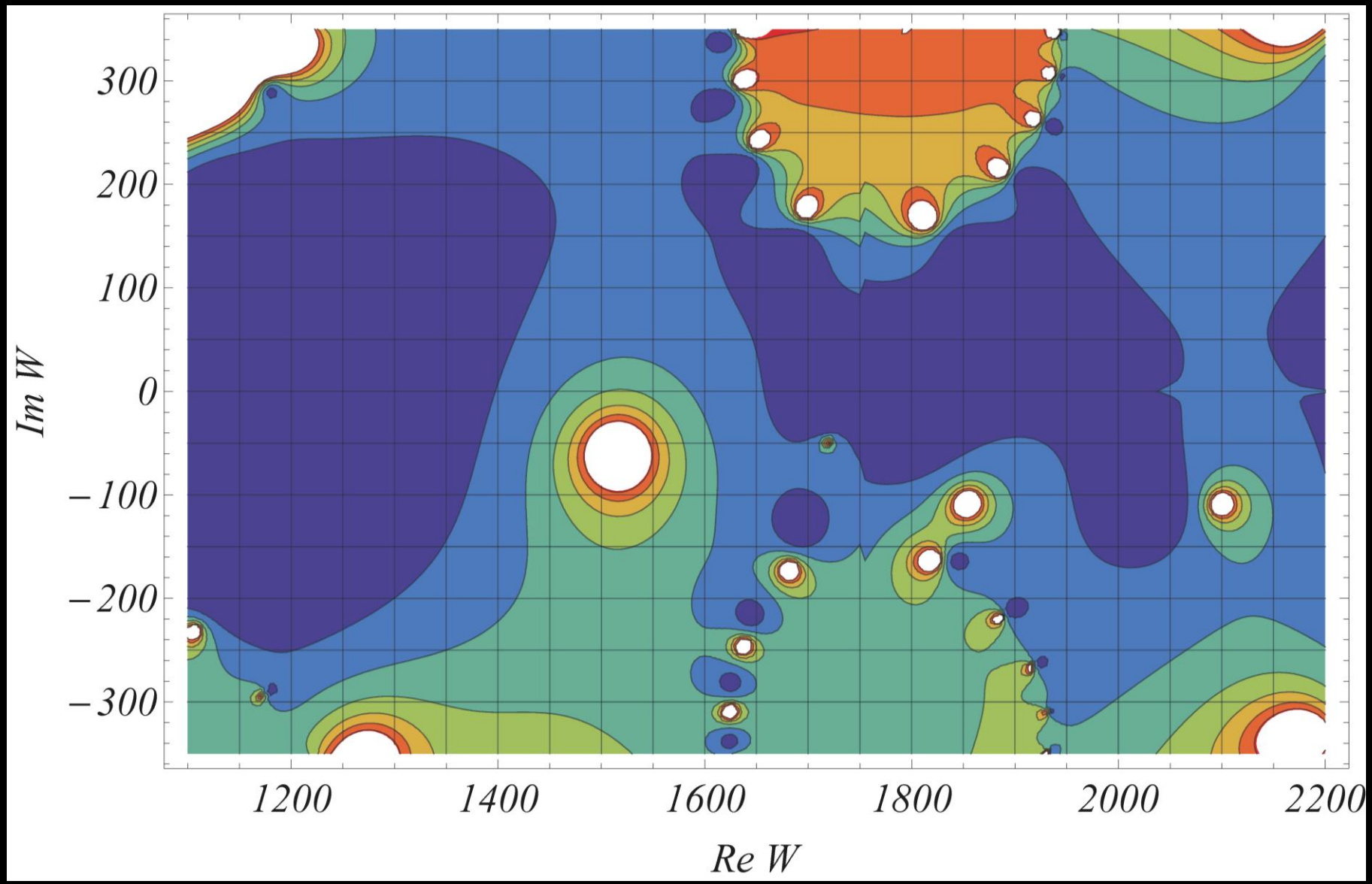

L+P expansion of energy-dependent (ED) solutions for γ,π

MAID2007
energy-dependent solution (ED)

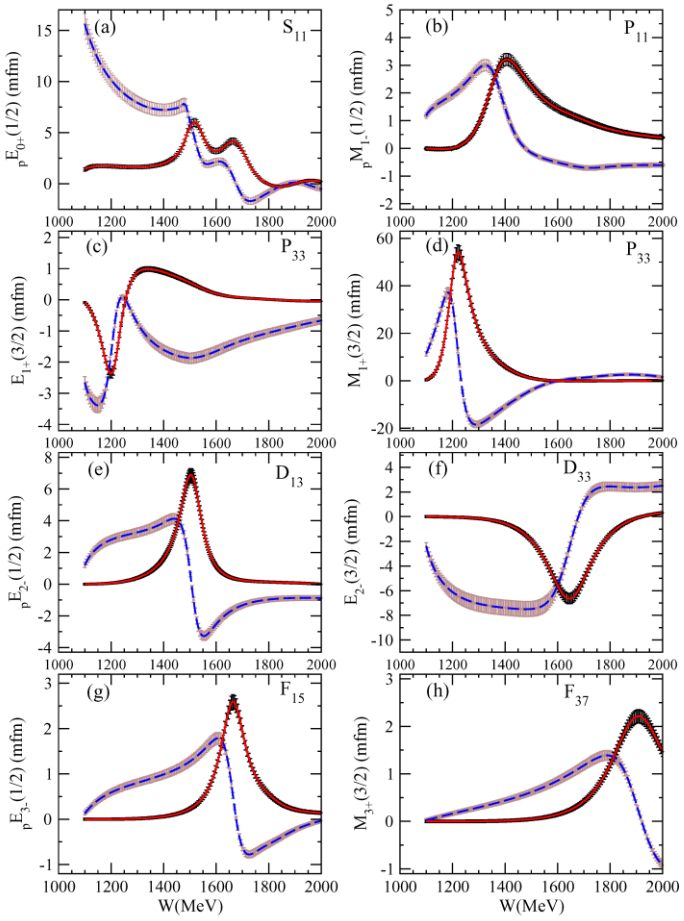

SAID CM12
energy-dependent solution (ED)

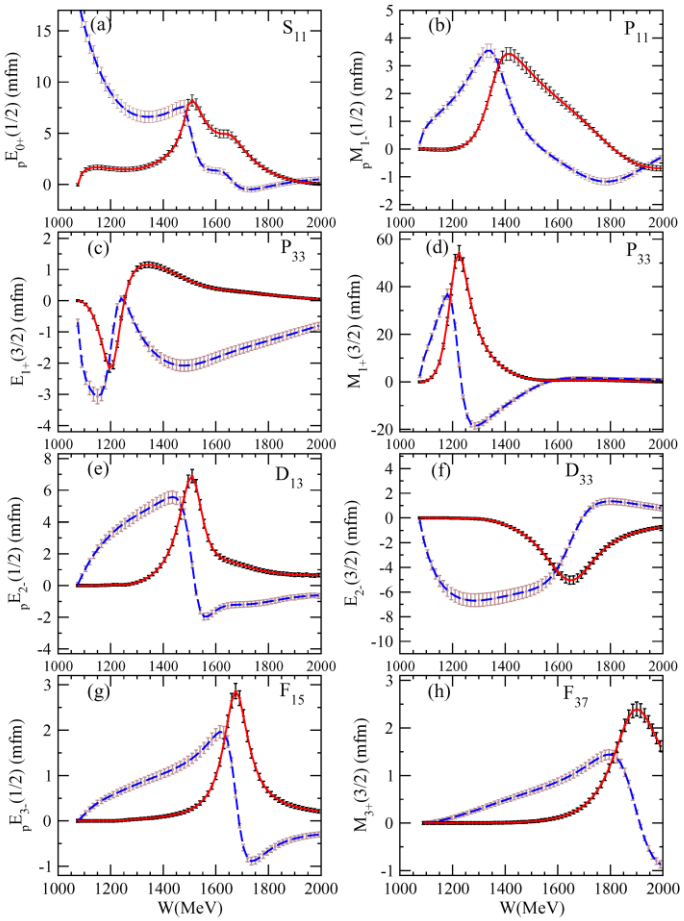

the L+P expansion of an ED solution is practically a numerical approximation of high accuracy

L+P expansion of single-energy (SE) solutions for γ,π

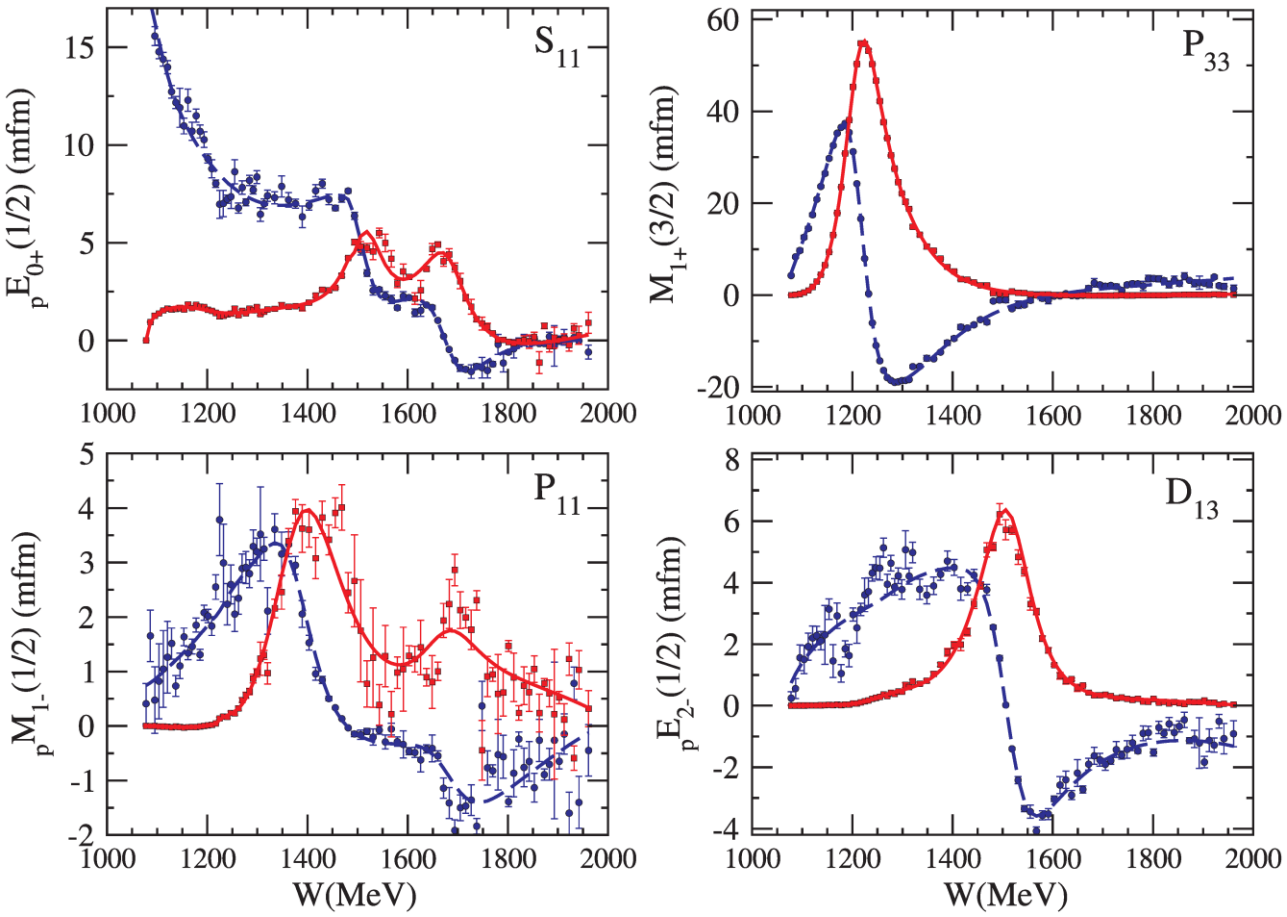

the L+P expansion of a SE solution is a χ^2 minimization

of a paramterization with the physical degrees of freedom

Only the (global) L+P method can deal with such single-energy data.
Methods, which depend on higher derivatives can not be applied here.

Resonance parameters from L+P expansion of γ,π amplitudes

from such Laurent+Pietarinen expansions

we get a whole set of model-independent resonance parameters

for many N* and Δ states

Multipole	Source	Resonance	Re W_p	-2Im W_p	|residue|	θ	$\|A_{1/2}\|$	$\|A_{3/2}\|$
$P_{33}(M_{1+})$	MAID	$\Delta(1232)3/2^+$	1210(1)	100(1)	3.010(23)	$-30(1)^\circ$	0.019(2)	0.133(2)
	SAID		1211(1)	101(1)	3.008(35)	$-27(1)^\circ$	0.028(4)	0.133(6)
$P_{11}({}_pM_{1-})$	MAID	N(1440)$1/2^+$	1379(6)	183(8)	0.394(8)	$-36(6)^\circ$	0.058(1)	–
	SAID		1367(10)	235(11)	0.547(58)	$-75(7)^\circ$	0.055(3)	–
$S_{11}({}_pE_{0+})$	MAID	N(1535)$1/2^-$	1511(7)	93(9)	0.210(23)	$-5(8)^\circ$	0.071(3)	–
	SAID		1501(3)	112(9)	0.312(25)	$-18(4)^\circ$	0.074(10)	–

Poles

on different Riemann sheets

Branch cuts in scattering amplitudes

$$T_{if}(W) = \frac{\sqrt{\Gamma_i \Gamma_f}/2}{M - W - i\,\Gamma/2} + b.g.(W)$$

in general, $\Gamma = \Gamma(W)$

$$\Gamma(W) = \frac{q_{\pi N}(W)}{q_{\pi N}(M)} \beta_{\pi N} \Gamma_{total} + \{\pi\pi N, \pi\Delta, \eta N + \cdots\}$$ for S wave

$$q_{\pi N}(W) = \frac{\sqrt{(W^2 - (m_p + m_\pi)^2)(W^2 - (m_p - m_\pi)^2)}}{2W}$$

$$= \sqrt{W - (m_p + m_\pi)}\sqrt{W + (m_p + m_\pi)}\sqrt{W - (m_p - m_\pi)}\sqrt{W + (m_p - m_\pi)}/2W$$

most important πN branch-point

in general: $\Gamma(W) \sim q^{2L+1}$, therefore this branch point exists in any partial wave

Square-Root function on 2 Riemann sheets

branch-cut to the left, standard in Fortran, C++ or Mathematica

$\Phi = -180^\circ$: SqrtL[z_] := $\sqrt{z}$

real part

imaginary part

1. Riemann sheet

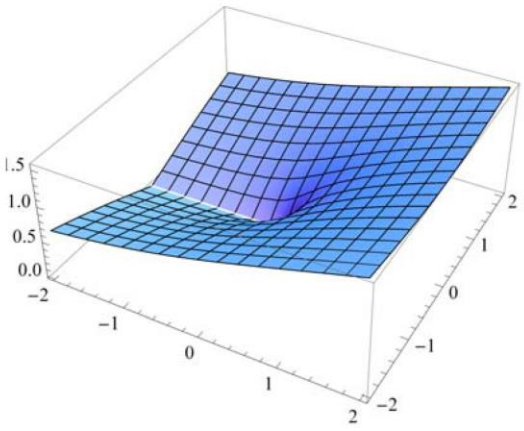

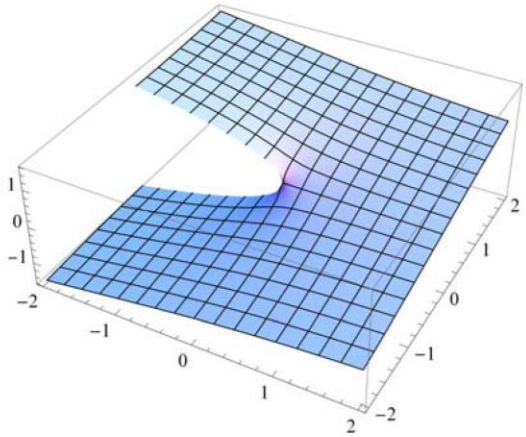

2. Riemann sheet

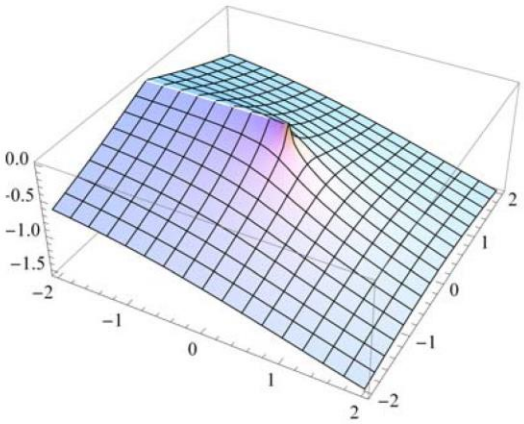

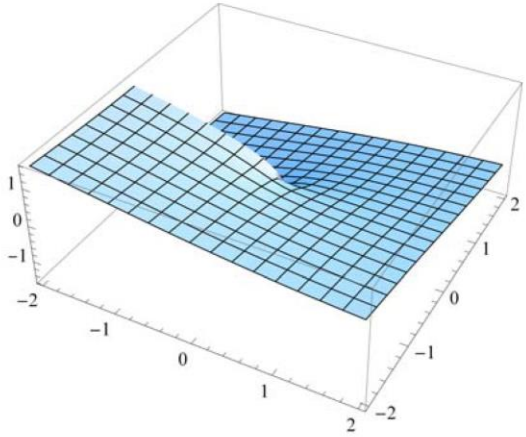

Redefinition of the square-root function

branch-cut to the left, standard in Fortran, C++ or Mathematica

$$\sqrt{-1 \pm i\varepsilon} = \pm i$$
$$\sqrt{-1} = +i$$

: the branch cut connects to the upper half-plane

in general, the branch cut can be rotated in any direction:

$\sqrt{z} \rightarrow \sqrt{z}$		branch-cut to the left	
$\rightarrow i\sqrt{-(z+i\varepsilon)}$	[1]	branch-cut to the right	standard way in particle physics
$\rightarrow \sqrt{i}\sqrt{-iz}$		branch-cut downwards	very convenient for pole analysis

[1] to meet the physics boundary conditions,
the branch-cut must always connect to the upper half-plane of the 1. Riemann Sheet

the square-root function on the 2. Riemann Sheet simply gets a minus sign in front

Square-Root function on 2 Riemann sheets with right-hand cut

branch-cut to the right, often used in particle physics

$$\Phi = 0^\circ \quad : \quad \text{SqrtR}[z\_] := +i\sqrt{-\left(z + i\,1.0\,10^{-15}\right)}$$

1. Riemann sheet

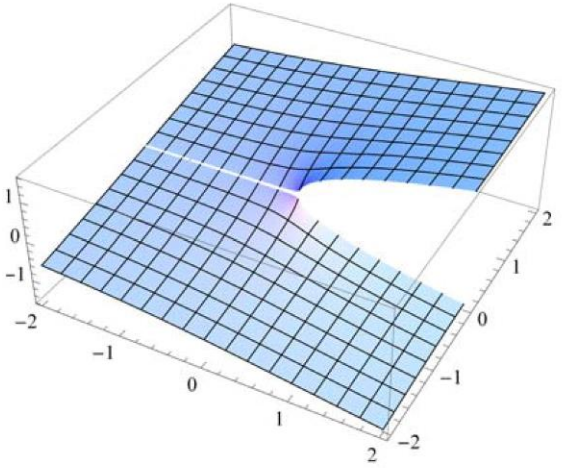

real part

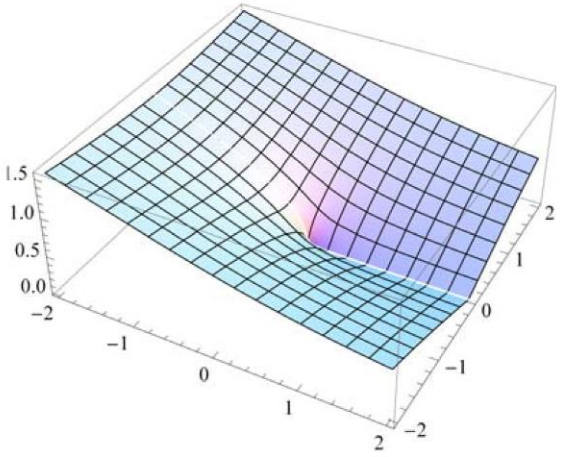

imaginary part

2. Riemann sheet

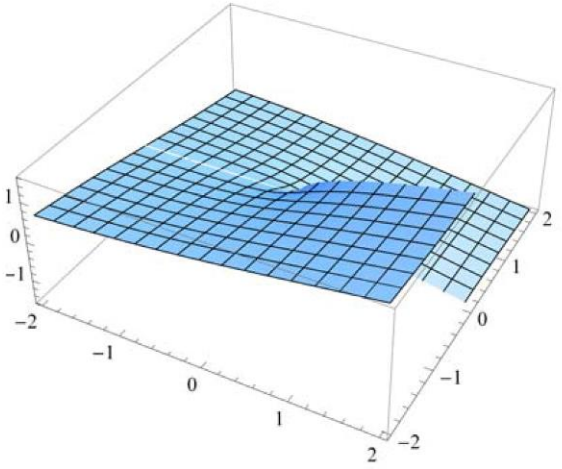

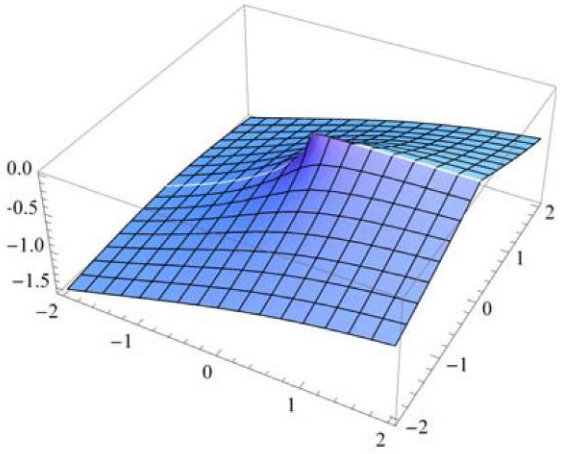

Delta(1232) on 2 Riemann Sheets

contour plots of the moduli of the T-matrix, $|T(W)|$

branch-cut to the left

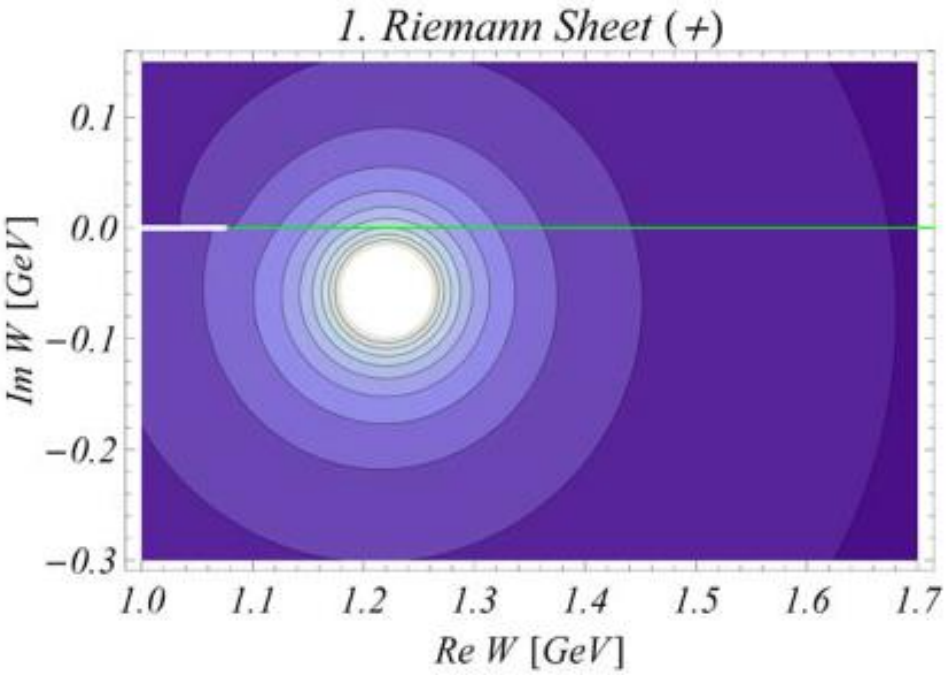

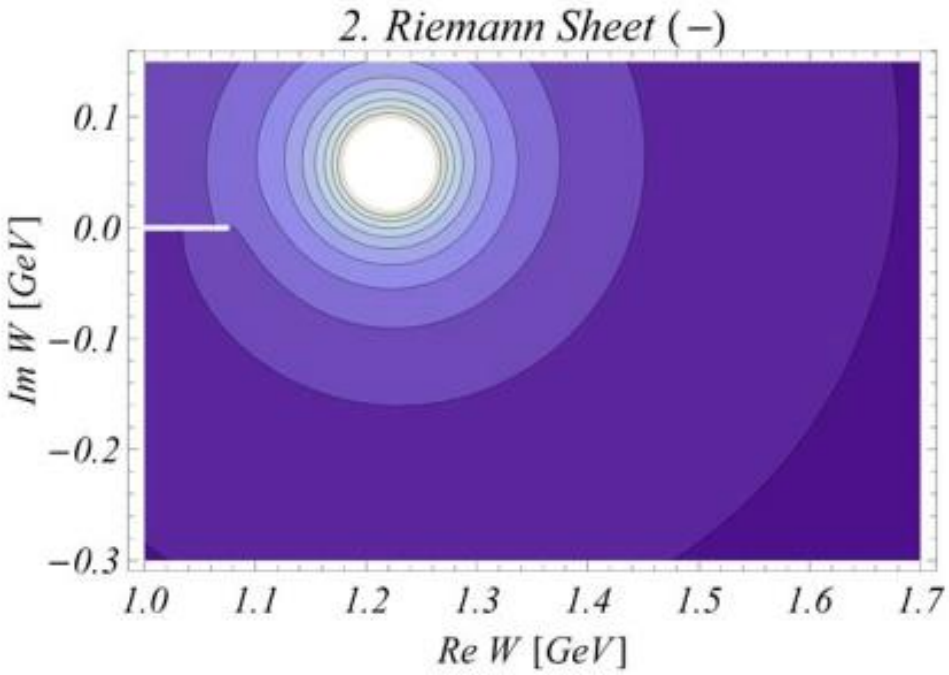

green line is the physical axis

Delta(1232) on 2 Riemann Sheets

branch-cut to the **left**

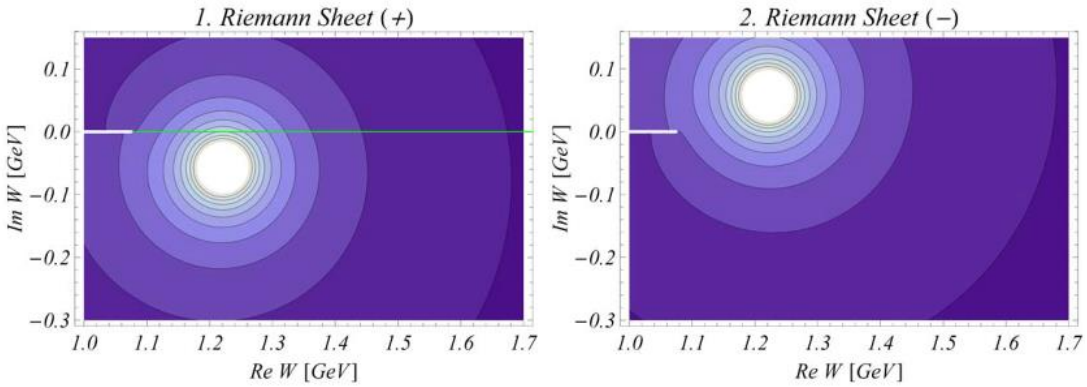

branch-cut to the **right**

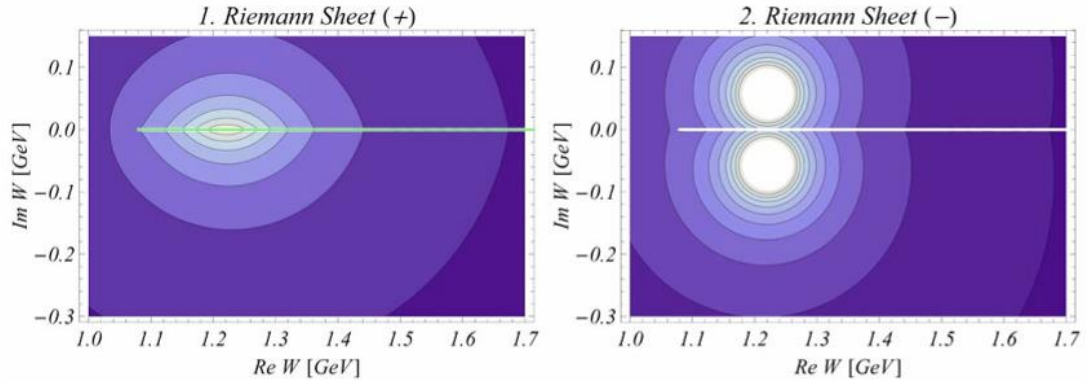

branch-cut **downwards**

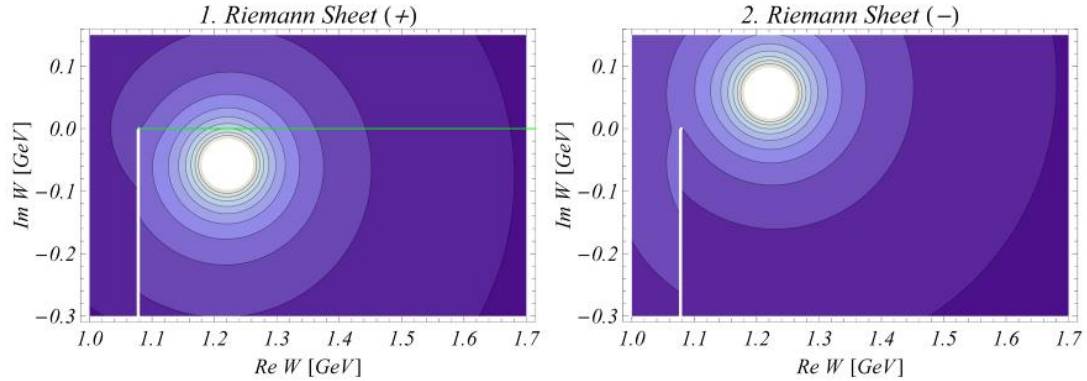

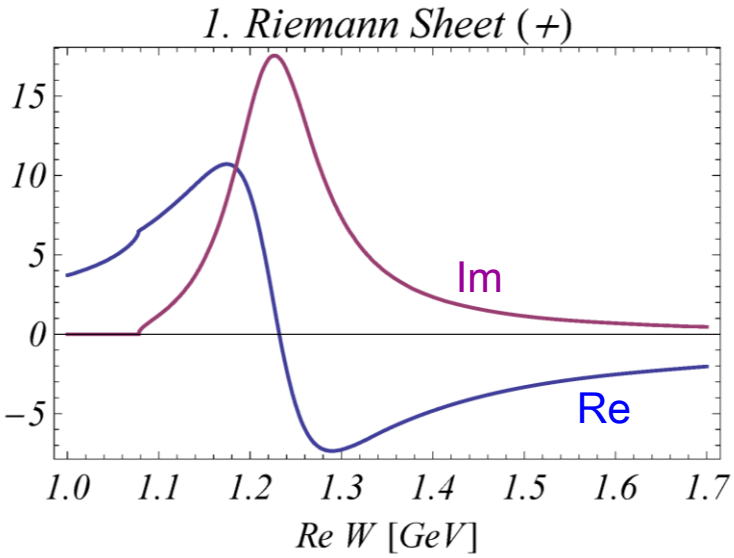

the amplitudes on the physical axis are always the same

<u>the only thing that counts:</u>

no pole in the

upper half-plane

of the 1. Riemann sheet

Delta(1232) on 4 Riemann Sheets

Δ(1232) on 4 Riemann sheets
with ππN channel

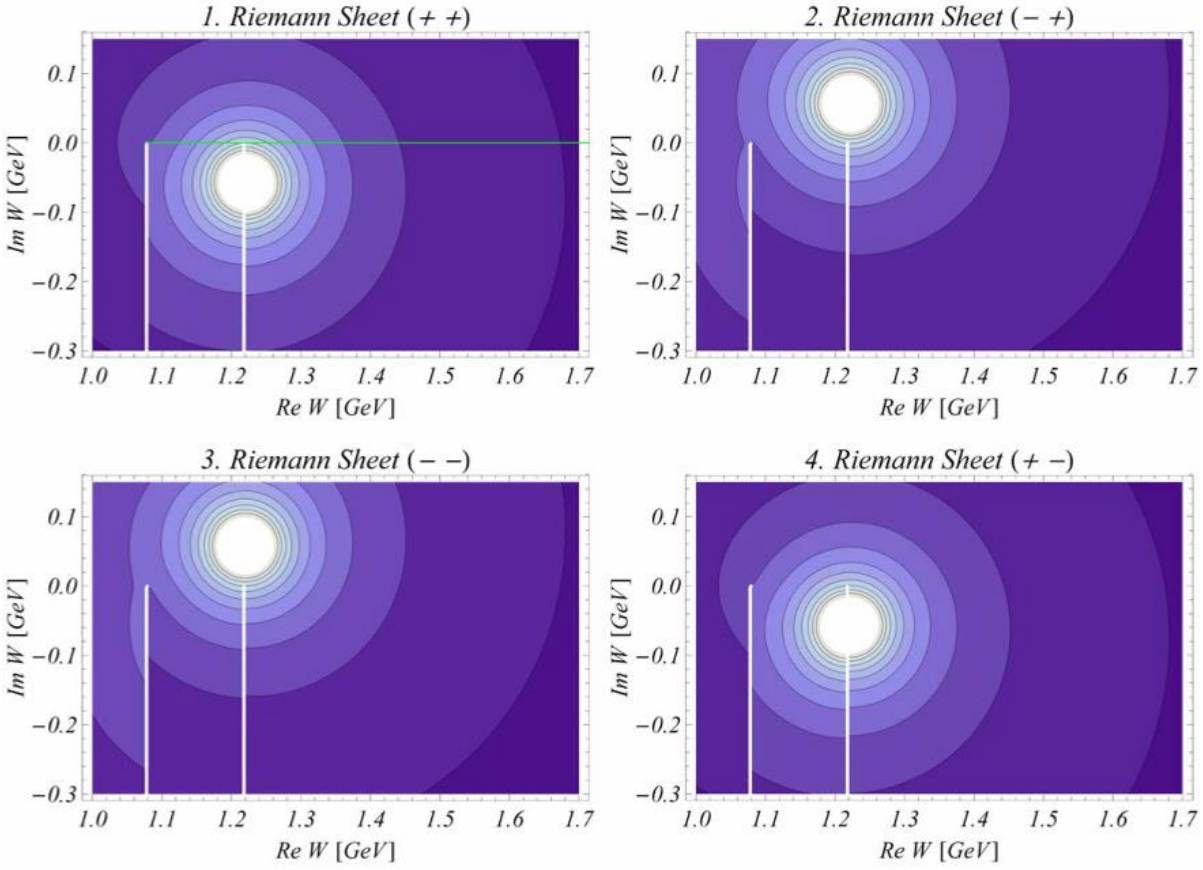

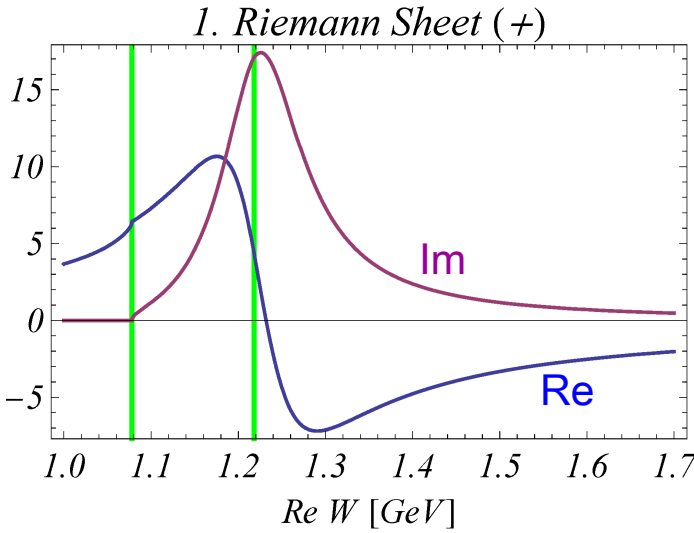

2 thresholds,
but second branch
is negligible

Roper(1440) and S11(1535) on 4 Riemann Sheets

(just for illustration, not very realistic, but typical pole scenario in dynamical models)

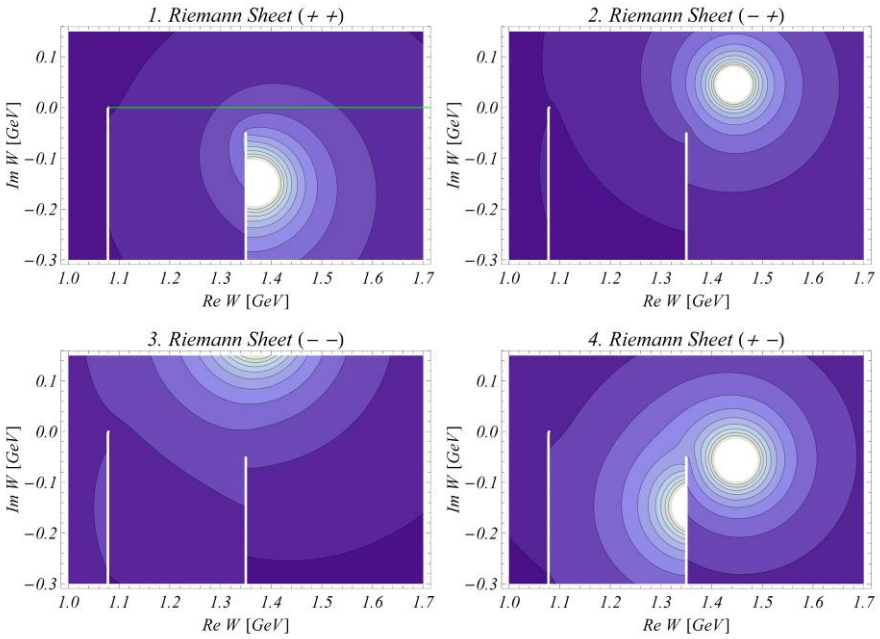

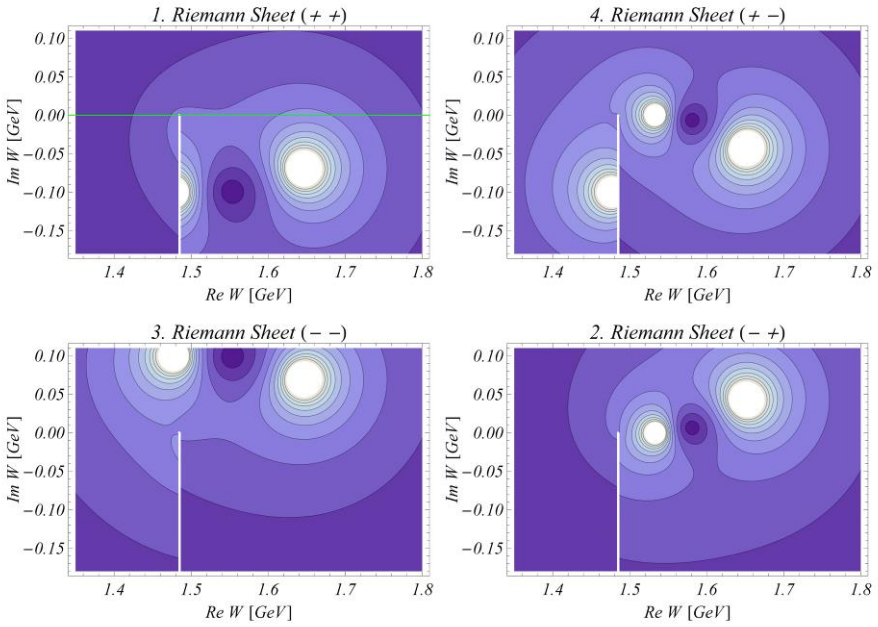

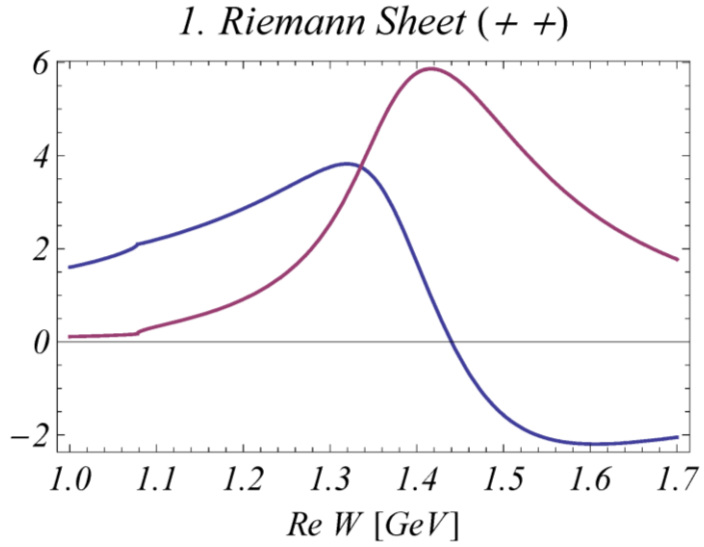

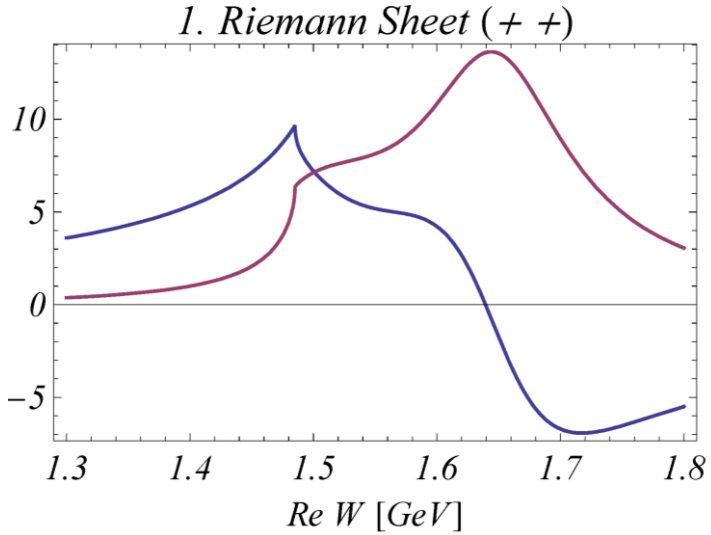

Lambda(1405) on 4 Riemann Sheets

$\Lambda(1405)$ is most famous example for a dynamically generated resonance

it couples to 2 channels:
$\pi\Sigma$ and $\bar{K}N$, which is only slightly above the dominant resonance pole

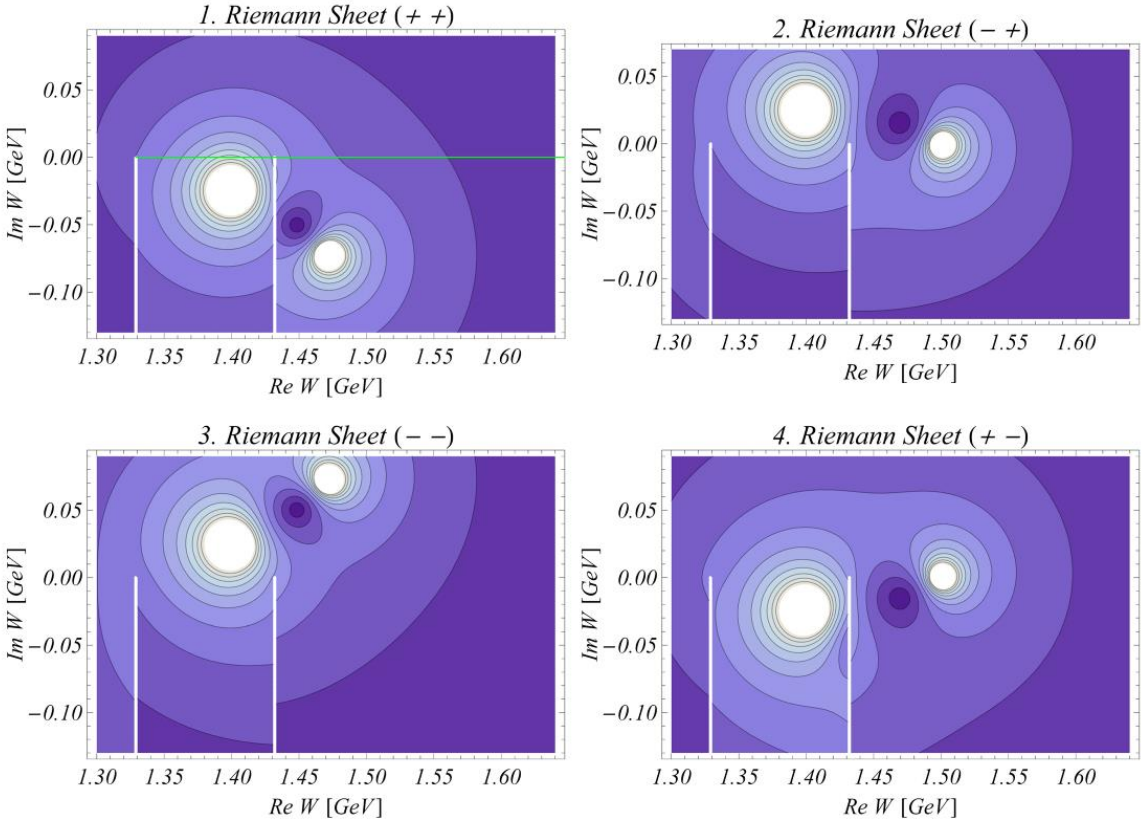

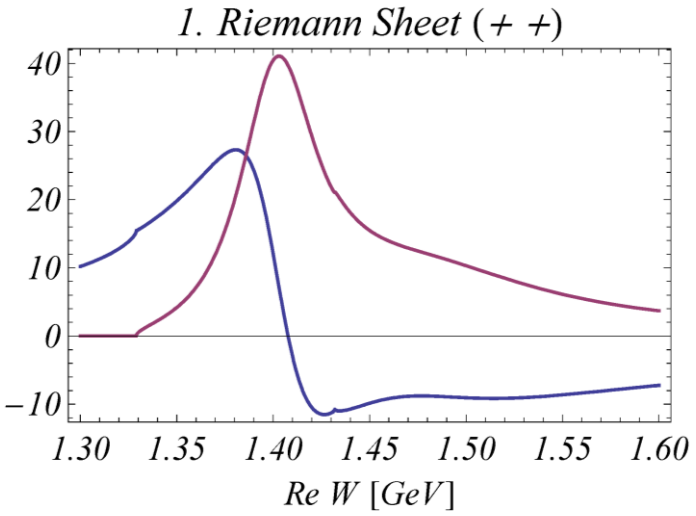

2 poles in $\Lambda(1405)$ region in real data analysis

M. Mai, U.-G. Meißner / Nuclear Physics A 900 (2013) 51–64

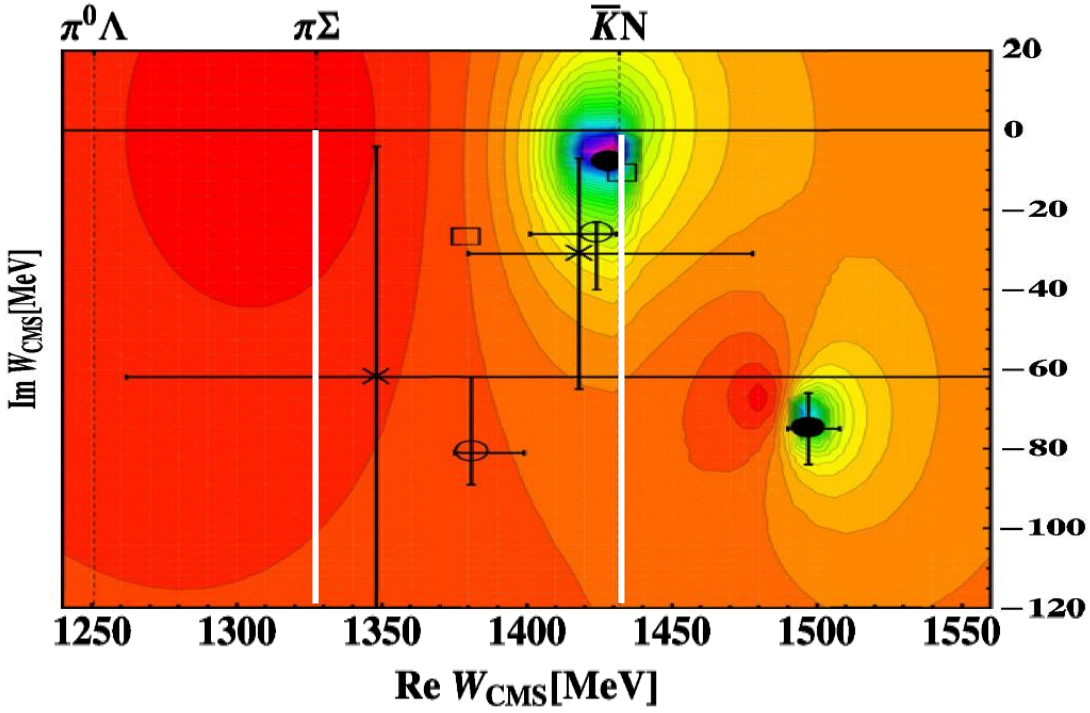

Fig. 5. Contour plot of the absolute value of the scattering amplitude for isospin $I = 0$ in the complex $W_{\rm cms}$ plane. Both Riemann sheets $\mathcal{R}_{\Sigma\pi}$ and $\mathcal{R}_{KN}$ are 'glued' together along the $\bar{K}N$ threshold line. The pole positions of comparable models are presented in the plot via squares [13], circles [6,7] and crosses [5].

Poles in Λ(1405) region from different analyses

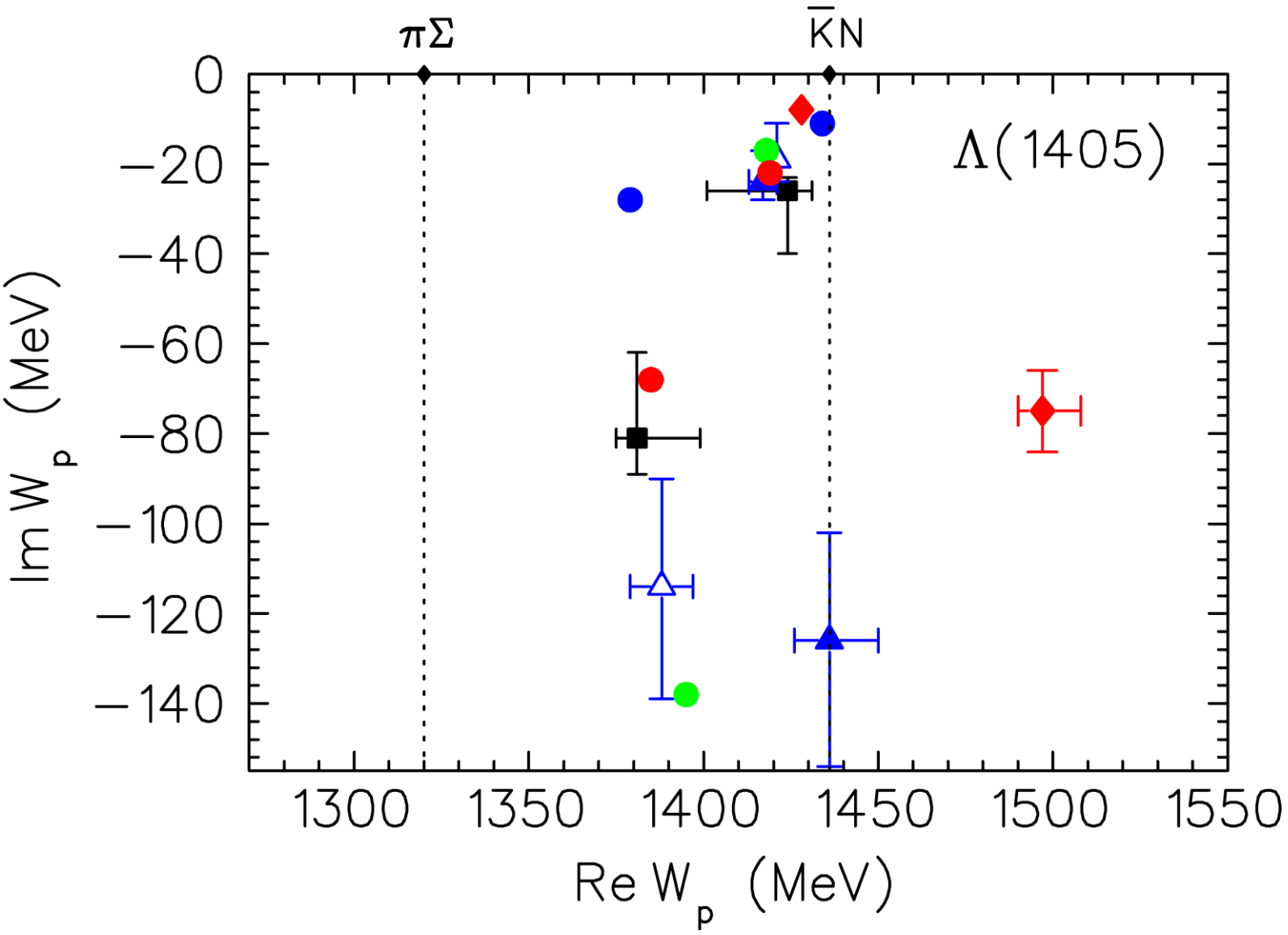

Pole positions of all 4* N and Δ resonances

from PDG2012 entries

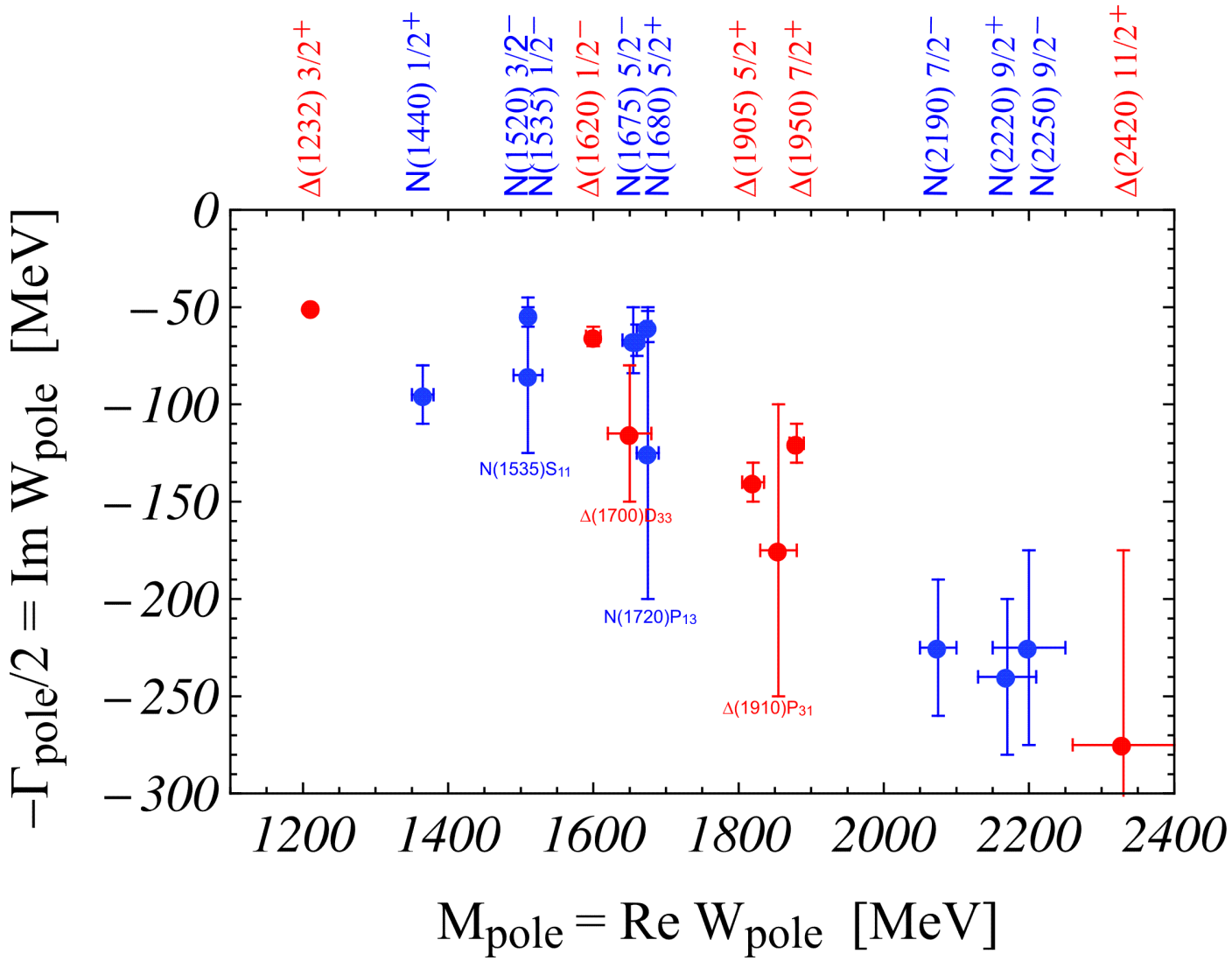

ENDE